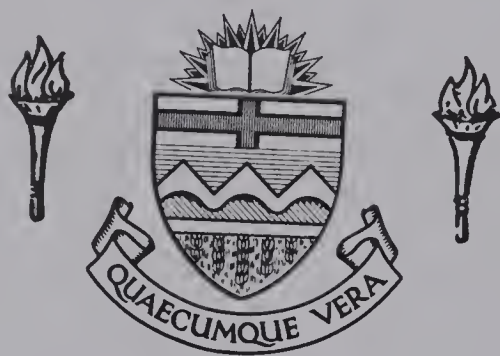


For Reference

NOT TO BE TAKEN FROM THIS ROOM

Ex libris
UNIVERSITATIS
ALBERTAEENSIS



THE UNIVERSITY OF ALBERTA

FLOTATION BEHAVIOR OF BARITE WITH ADSORBED FATTY ACIDS

by



Myung Kil Kim

A THESIS

SUBMITTED TO THE FACULTY OF GRADUATE STUDIES AND RESEARCH
IN PARTIAL FULFILMENT OF THE REQUIREMENTS FOR THE DEGREE
OF MASTER OF SCIENCE

DEPARTMENT OF MINING AND METALLURGY

EDMONTON, ALBERTA

SPRING, 1972

1422
1072
71

THE UNIVERSITY OF ALBERTA
FACULTY OF GRADUATE STUDIES AND RESEARCH

The undersigned certify that they have read, and recommend to the Faculty of Graduate Studies and Research, for acceptance, a thesis entitled "Flotation Behavior of Barite with Adsorbed Fatty Acids" submitted by Myung-Kil Kim in partial fulfilment of the requirements for the degree of Master of Science.

ABSTRACT

Collecting properties of fatty acid-type collectors for barite were extensively studied by employing various kinds of experimental techniques, such as zeta potential measurements, infrared spectroscopy and flotation tests. Through these experiments, it was established that there is a direct interaction between the collector hydrocarbon chain and the solid surface. Infrared spectroscopic studies on the adsorbed fatty acids showed that new carbon-carbon double bonds are formed in the first adsorbed layer at the expense of methylene groups. Association of collector species on the surface seems to proceed until both the attractive dispersion forces among hydrocarbon chains and the electrostatic repulsive forces among the ionic collector heads are balanced in the adsorbed multilayer. The conventional collector adsorption models, in which the hydrocarbon chains are oriented towards the liquid phase forming a compact monolayer on the solid surface, is thereby refuted for fatty acid-type collectors.

Based on the experimental results, a new adsorption model for fatty acid-type collectors is proposed. The new model assumes that the collector species are adsorbed parallel to the surface. This new model provides a reasonable explanation regarding the characteristic collecting properties of fatty acid-type collectors.

ACKNOWLEDGEMENT

The research work described in this thesis was carried out in the laboratories of the Department of Mining and Metallurgy under the supervision of Professor L.R. Plitt. The author greatly respects his scientific wisdom and values his friendship.

The author also enjoyed a congenial association with the other staff members of the department for which he is grateful. In particular, the author wishes to thank Dr. S.A. Bradford for his advice and many helpful discussions. The author also wishes to acknowledge the assistance and advice he obtained from the departmental technicians, particularly Mr. K.E. Hartung. The author is also indebted to Mrs. R. Mei for her efforts in typing this thesis.

Grateful acknowledgement is made to the National Research Council of Canada for the financial assistance given to the author during his Master's program.

TABLE OF CONTENTS

	<u>Page</u>
INTRODUCTION	1
THEORETICAL REVIEW	7
1. Properties of Fatty Acids	7
A. Structure	7
B. Dissociation	8
C. Acidity	9
D. Properties as a Collector	10
2. Adsorption Mechanism	12
A. Adsorption at Solid-Liquid Interfaces	12
B. Collector Adsorption Theory	16
C. Hemimicelle Hypothesis	21
D. Adsorption Mechanisms of Fatty Acids	24
3. Electrokinetic Phenomena at Solid-Liquid Interfaces	26
A. Electrical Double Layer	26
B. Structure of the Electrical Double Layer	31
C. Significance of Surface Potential in Flotation	34
EXPERIMENTAL METHODS	37
1. Materials	37
A. Reagents	37
B. Sample	38
2. Apparatus and Procedures	40
A. Hydrogen Ion Adsorption Measurements	40
B. Mobility Measurements	40

	<u>Page</u>
C. Infrared Transmission Techniques	42
D. Modified Hallimond Tube Tests	44
EXPERIMENTAL RESULTS AND DISCUSSION	47
1. Electrokinetic Surface Phenomena	47
A. Variation of Zeta Potential as a Function of pH	48
B. Variation of Zeta Potential in Different Electrolyte Solutions	55
2. Infrared Studies on Adsorbed Fatty Acids	58
A. C-H Stretching Vibrations	58
B. Infrared Spectra of Various Kinds of Fatty Acids Adsorbed on Barite	60
C. Infrared Spectra of Adsorbed Oleate in Different Concentrations	63
D. Infrared Spectra of Adsorbed Oleate at Different pH Levels	65
3. Flotation Experiments	67
A. Flotation Recovery of Barite as a Function of the Concentration of Various Fatty Acids	68
B. Effects of pH on the Recovery of Barite	71
4. New Adsorption Model for Fatty Acid-Type Collectors	73
SUMMARY AND CONCLUSIONS	77
REFERENCES	80
APPENDIX A	85
APPENDIX B	91

LIST OF FIGURES

	<u>Page</u>
Fig. 1. Schemetic Diagram of Alkyl and Carboxyl Group	7
Fig. 2. Collector Adsorption Models	19
Fig. 3. Collector Ion Association on a Solid Surface	22
Fig. 4. Electrical Double Layer Around a Solid Particle	30
Fig. 5. The Effect of the Electrolyte Concentration and Valency on the Electric Potential	30
Fig. 6. Potential Variation in Different Electrical Double Layer Structures	32
Fig. 7. Sample Preparation Procedures	39
Fig. 8. Apparatus for Electrophoretic Measurement	41
Fig. 9. Flotation Apparatus	45
Fig. 10. Variation of Zeta Potential of Barite and Quartz as a Function of pH	49
Fig. 11. Hydrogen Ion Adsorption on Barite and Quartz	53
Fig. 12. Variation of Zeta Potential as a Function of the BaCl_2 Concentration	56
Fig. 13. Variation of Zeta Potential as a Function of Na-Oleate Concentration	57
Fig. 14. Typical Infrared Spectrum of an Unsaturated Fatty Acid	59
Fig. 15. Infrared Spectra of N-saturated Fatty Acids Adsorbed on Barite	61

Fig. 16.	Infrared Spectra of C-18 Fatty Acids with Various Number of Double Bonds in Their Hydrocarbon Chain	62
Fig. 17.	Infrared Spectra of Na-Oleate Adsorbed on Barite in Different Concentrations	64
Fig. 18.	Infrared Spectra of Na-Oleate Adsorbed on Barite at Different pH values	66
Fig. 19.	Flotation Recovery of Barite as a Function of the Concentration of n-saturated Fatty Acids	69
Fig. 20.	Flotation Recovery of Barite as a Function of the Concentration of Unsaturated Fatty Acids with 18 Carbon Atoms	70
Fig. 21.	Flotation Recovery of Barite as a Function of pH	72
Fig. 22.	Schematic Diagrams of Collector Conditioned Solid Surfaces and Air Bubble Attachment	74

EQUIVALENT NOTATION USED IN TEXT

ACS : American Chemical Standard

C : Concentration

D : Dielectric constant

D.C. : Direct current

DD Water : Demineralized-distilled water

d : Diameter of a particle

E : External potential

HX : Neutral collector molecule

I.R. : Infrared

K_a : Equilibrium constant

K_h : Hydrolysis constant

L : Litre

LCAO : Linear combination of atomic orbitals

M : Mole

ppm : Part per million

R : Alkyl group

S : Solid surface

S.S. Rod Mill : Stainless steel rod mill

v_e : Electrophoretic mobility

X⁻ : Collector anion

zpc : Zero point of charge

ζ : Zeta potential

ψ : Electric potential

ψ_o : Surface potential

μ : Micron

η : Absolute viscosity

τ : Double layer thickness

ν : Wave number

ρ : Charge density

INTRODUCTION

In recent years, the beneficiation of barite has acquired increased attention. Barite is characterized by its chemical stability, high specific gravity (about 4.5) and relatively low cost. Most of the barite mined is used as a weighting ingredient in oil well drilling muds. Barite is also used as a filler in paint, rubber, linoleum, and in the paper industry.

Barite is produced in large quantities in Canada. The principal Canadian production is from Walton, N.S., which is reported to contain a large reserve. Two deposits are also worked at Parson and Brisco, B.C., and barite is recovered from old mine tailings at Spillimacheen, B.C. Occurrences are known in other parts of Canada. Canadian production in 1970 was about 240,000 tons valued at \$2.1 million.⁽³⁰⁾

The beneficiation of barite is usually done by gravity separation methods. Gravity separation however has proven to be unable to produce a high grade of barite concentrate with a reasonable recovery. Therefore, in recent years, consideration is given to the beneficiation of barite by flotation.

In practical flotation systems, minerals are classified according to their flotation properties as follows:⁽²⁵⁾

a. Sulphides of Heavy Metals and Native Metals - This group contains minerals of copper, lead, zinc, mercury, antimony and others. Xanthates (dithiocarbonates) are the

most effective collectors for the flotation of these minerals.

b. Non-polar, Non-metallic Minerals - Graphite, sulphur, coal and talc belong to this group. Flotation concentration of these minerals requires utilization of extremely weak collectors and sometimes only frothers.

c. Oxidized Minerals of Non-ferrous Metals - Carbonates and sulfates of copper, lead, and zinc (cerussite, anglesite, smithsonite, malachite, azurite, wulfenite, etc.). Minerals of this group can be floated by xanthate collectors after their sulphidization. These minerals can also be floated by fatty acids and their soaps.

d. Polar Salt-type Minerals which Contain Cations of Calcium, Magnesium, Barium and Strontium - Minerals in this group are scheelite, apatite, phosphorite, fluorite, calcite, barite, magnesite, dolomite, etc. These minerals are easily floated with anionic collectors such as fatty acids.

e. Oxides, Silicates and Aluminosilicates - The following minerals belong to this group: silica, corundum, diaspore, gibbsite, zircon, rutile, hematite, magnesite, cassiterite, ilmenite, feldspars, mica, asbestos, tourmaline and kaolinite. A large number of minerals of this group possess good flotability when either anionic or cationic collectors are used. However, the flotability of many of these minerals with anionic collectors is directly related to the presence of activating cations in their surfaces and,

depending on the concentration of the latter, the flotability varies within wide limits for the same mineral.

f. Soluble Salts of Alkali and Alkaline Earth Metals - minerals of this class, amenable to flotation are halite, sylvite, langbeinite, kyanite, etc. These salts can be floated in their saturated solution either by means of fatty acids or collectors of the cationic type.

Separation among minerals which belong to different groups can be done easily by flotation in most of the cases. However, difficulties are encountered where separation is required among minerals of the same group. Selective flotation among commonly associated sulfide minerals is better established than for the salt-type minerals and the silicates. The flotability of these kinds of non-sulfide minerals is affected by many factors, such as crystal structure, presence of impurities, and origin.⁽⁴⁰⁾ Knowledge of the basic mechanism of adsorption of collectors on different mineral surfaces, therefore, is essential to understand the characteristic flotation behavior of minerals.

Fatty acids are the most widely used collectors for non-sulfide mineral flotation. Under proper conditions, these collectors have the tendency to float nearly all minerals. In the past, fatty acid collectors were even used for sulfide mineral flotation before more effective collectors, such as xanthates and dithiophosphates, were discovered in 1925. In fact, the first commercial application of flotation in North America at Basin, Montana in 1911, used a

fatty acid collector to produce a sphalerite concentrate.⁽¹²⁾ Because of their non-selectivity, close control of the flotation conditions is necessary to obtain good mineral separation, when fatty acid type collectors are employed.

The function of fatty acid as a collector in non-sulfide mineral flotation circuits has been studied by numerous workers. In 1950, Eigeles⁽²⁵⁾ made a detailed study of the collecting properties of oleic acid. He studied how the nature of mineral, the concentration of reagents, the time of contact and the temperature affect the adsorption of collector on the non-sulfide mineral surfaces. The fundamental mechanisms regarding adsorption of collector on a mineral surface were not included in his studies. Basic principles and quantitative description about these kinds of surface reactions are still beyond our complete understanding. However, the recent development of other branches of surface chemistry and new experimental techniques make it now possible to make closer predictions about the flotation behavior of a specific mineral and the collector adsorption mechanisms.

Generally employed experimental techniques may include contact angle and surface area measurements, radioactive tracers, electron microscopy, X-ray diffraction, chemical determination of adsorption isotherms, and electrochemical methods of investigation. From these kinds of experiments, wettability, the orientation of adsorbed species, mono- or multi- layer type adsorption, and distri-

bution of collector on the mineral surfaces have been described. These techniques, however, have proven incapable of determining the specific nature of the adsorbed collector film.

In recent years, infrared spectroscopy has proven to be the most useful tool available for the solution of problems having to do with molecular structure, molecular behavior, and identification of unknown organic chemical substances. Since an infrared spectrum represents the vibrational and rotational modes of chemical bonds in a molecule, this method can be used in studying molecular interactions at both solid/gas⁽⁸⁾ and solid/liquid⁽¹⁰⁾ interfaces.

Mechanisms involved in the adsorption of oleic acid and sodium oleate on the surface of three commonly associated minerals, fluorite, calcite and barite were studied using infrared techniques by Peck and Wadsworth.⁽³²⁾ Evidence was presented that the collector chemisorption reactions displace anions from the mineral surfaces and form corresponding metal-oleate salts. This investigation showed that the addition of these ions which serve as the building blocks of a mineral, sharply depress the formation of the chemisorbed oleate species. Explanations regarding development of hydrophobicity on a mineral surface by adsorbing collector species was not explained in their studies.

In the studies described in this thesis, efforts were made to understand the characteristic surface behavior

of natural barite in a flotation system, and the collecting properties of fatty acids through the use of different experimental techniques.

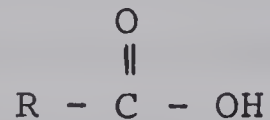
The experimental techniques employed in this study included hydrogen ion adsorption, mobility and flotability measurements for barite. Several experiments were also conducted using quartz in order to understand the differences in flotation properties between salt-type and silicate minerals. Infrared spectra were used to identify the specific nature of the adsorbed collector species.

THEORETICAL REVIEW

1. Properties of Fatty Acids

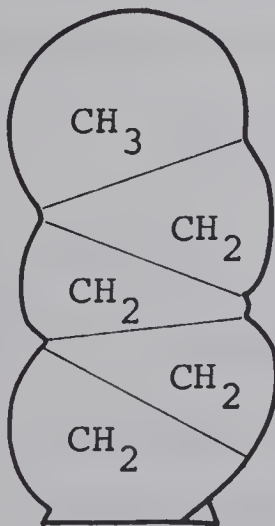
A. Structure

The structural formula of fatty acids may be expressed such as:

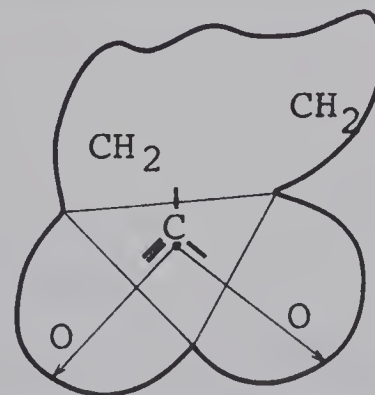


where 'R' represents an alkyl group. The 'H' can be replaced by a monovalent metal ion forming a soap.

Fig. 1 shows schematically the structure of the hydrocarbon chain consisting of CH_3 and CH_2 groups and the carboxyl group.



a. Hydrocarbon Chain

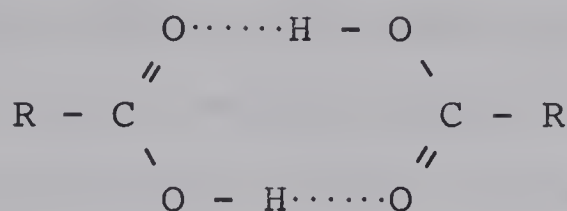


b. Carboxyl Group

Fig. 1. Schematic Diagram of Alkyl and Carboxyl Group (25)

As can be seen from their structure, fatty acid molecules are composed of a polar carboxyl group and a nonpolar alkyl group. Fatty acids form hydrogen bonds with each other, or with other kinds of molecules such as alcohol.

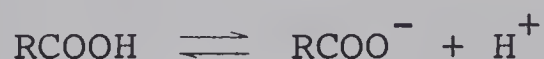
The hydrogen bond formation of fatty acids is shown below:



Fatty acids have higher boiling points than alcohols having the same carbon length because fatty acid molecules are bound together by two hydrogen bonds whereas alcohol molecules are joined with only one hydrogen bond.

B. Dissociation

In aqueous solution, the fatty acid molecules exist in equilibrium with the carboxylate anions and the hydrogen ions illustrated as follows: (25)



denoting the equilibrium constant of above reaction as K_a , the concentration of carboxylate anion in solution is given:

$$[\text{RCOO}^-] = K_a \frac{[\text{RCOOH}]}{[\text{H}^+]}$$

since, $[\text{H}^+] = 10^{-\text{pH}}$, therefore,

$$[\text{RCOO}^-] = K_a [\text{RCOOH}] 10^{\text{pH}} \text{ (mole/litre)}$$

For the alkali salt of a fatty acid, the concentration of the carboxylate anion in a solution depends very much on the hydrolysis of carboxylate anion:



Hence, the concentration of carboxylate anion is equal to:

$$[\text{RCOO}^-] = \frac{[\text{RCOOH}] [\text{OH}^-]}{K_h}$$

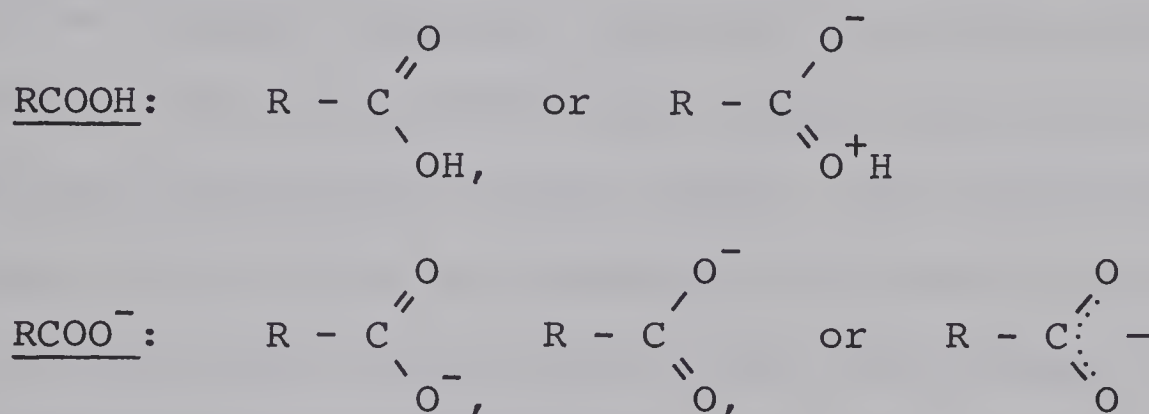
$$\text{Or, } [\text{RCOO}^-] = \frac{1}{K_h} [\text{RCOOH}] 10^{(\text{pH}-14)} \text{ (mole/litre)}$$

here K_h is the hydrolysis constant.

The above equations show that regardless of whether fatty acids or their alkali salts are in solution, the concentration of carboxylate anions depends upon the pH. The concentration of carboxylate anions increases as the pH of the solution is increased.

C. Acidity

The acidity of a fatty acid in solution is determined by the difference between the stability of the undissociated acid and its anion.⁽³¹⁾ Two reasonable structures for both the fatty acid and its carboxylate anion can be drawn as follow:



As shown above, both the acid and the anion are resonance hybrids. As a result of this resonance hybrid structure, both acid and anion are stabilized. The stabilization is expected to be far greater for the anions than for the acids because the anion has an exactly symmetrical structure.⁽³¹⁾

In a carboxylate anion, the carbon atom is joined to the three other neighboring atoms by hybridized bonds. Since these bonds utilize sp^2 hybridized orbitals, they lie in a plane at an angle of 120° . The remaining p orbital in the carbon atom overlaps equally on the p orbitals of both oxygens, and forms hybrid bonds. In this way, the electron

is not bonded just to one or two nuclei but to three (one carbon and two oxygen atoms). Because of this resonance structure, the two oxygen atoms are held more tightly, making the anion more stable than the molecule. This stabilization of the anion and resulting acidity are only possible because of the presence of the carbonyl group in a fatty acid molecule.

The structure of the alkyl group in a fatty acid molecule has pronounced effects on its acidity. Any factor that stabilizes the anion more than the acid should increase acidity. Electron-withdrawing substituents should disperse the negative charge, stabilize the anion, and thus increase the acidity. For n-saturated fatty acids, the acidity is increased with decreasing carbon length. For unsaturated fatty acids, the acidity is increased by increasing the number of double and triple bonds in the hydrocarbon group.

D. Properties as a Collector

The length and the structure of the hydrocarbon chain in a fatty acid molecule has a pronounced effect on its collecting properties.

For n-saturated fatty acids, the solubility is decreased 3 to 3.2 fold (Traube's Rule⁽¹⁶⁾) for each additional carbon atom. The collecting power is increased with increasing the number of carbon atoms in the hydrocarbon chain. However, fatty acids with very long hydrocarbon chain (above C-18) are so slightly soluble in water that their effectiveness as a collector is sharply decreased.

Fatty acids form very insoluble compounds with any di- and tri-valent cations. Therefore, in the presence of ions such as calcium, magnesium, iron, etc., the amount of collector needed in a flotation circuit is greatly increased.

Another important property of fatty acids in a flotation system is their tendency to form micelles in solution. About 650 calories of energy is evolved when one CH_2 group is removed from water.⁽¹²⁾⁽³⁸⁾ Because of this hydrophobicity, the fatty acid ions will aggregate to form colloidal-sized groups known as micelles. In a micelle, the hydrocarbon chains are removed from water by tight association of the chains inward and with the charged heads oriented outward towards the water.⁽¹²⁾⁽¹⁷⁾ A micelle attracts a fairly large number of ions to its surface as counter ions, which reduces its charge considerably. Therefore, the formation of a micelle in solution results in a sharp drop of the electrical conductivity of a solution when compared with a solution with an equivalent amount of other ions. The concentration at which micelles begin to form (critical micelle concentration) depends on the nature of the polar group and on the length of the hydrophobic radical. The formation of micelles is favored by increasing the hydrocarbon length due to an increase in dispersion forces between the longer hydrocarbon chains. This dispersion force is inversely proportional to the fifth power of the distance between the chains and directly proportional to the length of hydrocarbon chain.⁽²⁵⁾

In order to change a hydrophilic mineral surface to a hydrophobic surface, aggregation of collector ions on the mineral surface is essential. Furthermore, the arrangement of collector on the mineral surface is also regarded as a governing factor for a mineral to obtain hydrophobicity. An aggregation of collector ions at the surface of mineral is called a hemimicelle. Gaudin showed⁽¹⁷⁾ that the flotation recovery is greatly improved when collector ions start to form hemimicelles on a mineral surface.

Fatty acid type collectors give good flotability to all polar salt-type minerals which contain alkaline earth metals (calcium, magnesium, barium and strontium), and also to the carbonates and sulfates of non-ferrous metals. These collectors are not actively adsorbed on oxide minerals (silicates and alumino-silicates) without the presence of activating metal cations in the solution.

2. Adsorption Mechanism

A. Adsorption at Solid-Liquid Interfaces

Adsorption is a very complex phenomenon. Forces exist between molecules and a solid surface and also among the adsorbed molecules themselves. All intermolecular forces have their origin in the electromagnetic interactions of nuclei and electrons.⁽⁴⁾ Distribution of these forces can be determined, in principle, from their mutual interactions and the procedures of quantum mechanics, leading to a complete knowledge of the quantum mechanical states of the system. Such procedures are, however, too complex for

application even to the simplest of adsorption systems. Therefore, simplifications must be introduced. One simplification is to classify forces into those associated with physical adsorption and chemisorption. Distinction between physical adsorption and chemisorption, however, is not so simple. In most of the cases, physical adsorption is weaker than chemisorption and experimentally-determined heats of adsorption are often used to distinguish between the two types of adsorption.

Physical Adsorption: Physical adsorption results from the action of van der Waals forces which are considered to be made of the London dispersion forces and the classical electrostatic forces.⁽⁴⁾ In 1930, London was the first to recognize the existence of dispersion forces between atoms and molecules. According to the quantum mechanical theory developed by London, the electrons in atoms and molecules are in continuous motion even when they are in their ground states. Thus they possess rapidly fluctuating dipole moments, and fleeting dipole moments in one atom or molecule perturbs a neighboring one inducing a moment in it. The temporary moment in the first molecule and the moment induced in the neighboring one lead to an attractive force between them.

A prime example of attractive interactions consisting almost exclusively of dispersion forces is found in a system of non-polar molecules adsorbed on the surface of a covalent solid. Dispersion and electrostatic forces are the major attractive forces in systems of polar molecules adsorbed on

the surfaces of covalent solids, and spherically symmetrical inert atoms adsorbed on the surfaces of ionic solids.

Electrostatic forces interacting between non-polar molecules and ionic solids are generated by the polarization of the atom in electric fields of the ionic lattice. Polarization is a distortion of the electronic charge density around an ion and it can arise from a variety of inter-related causes. In its most extreme form, polarization results in the effective removal of an electron from an anion towards a cation and forms a covalent bond. Polarization can thus be considered as the link between purely ionic interaction on the one hand and purely covalent bonding on the other. Polarization is more extensive the lower the coordination number⁽²⁰⁾ and it also depends on both the polarizing power and the polarizability of the ions in the structure. Polarizing power increases with a decrease in ion radius and an increase in its charge. The less effectively the ion's nucleus is shielded by the extra-nuclear electrons the greater will be its polarizing power. Small, highly charged cations therefore have considerable polarizing power and d^{10} ions are more highly polarizing than inert gas type ions. By contrast, polarizability, or ease of distortion, will be greater for large ions (usually anions) with loosely bonded electrons.

Physical adsorption cases may include unionized molecules and ions held close to the surface of solid by the dispersion and the electrostatic forces. In this physical

adsorption, there is no transfer or sharing of electrons between the adsorbates and the adsorbents. As an adsorbate approaches the adsorbent, electrons may take up a new equilibrium distribution, but they maintain their respective associations in the interacting species.

Chemisorption: Simply stated chemisorption arises from the transfer or the sharing of electrons between an adsorbate and an adsorbent. The type of a chemical reaction that causes chemisorption includes most of the well recognized reactions familiar in bulk chemistry. That is, they probably involve simple addition reactions, complex chelation reactions, acid-base neutralization reactions, metathesis reactions, and perhaps even precipitation of neutral substances on the surface of a solid. These chemical reactions are believed not to proceed beyond the formation of a mono-layer on the surface.⁽³⁾

The simplest way of describing chemical forces of adsorption at solid surfaces, employs analogies with simple chemical bonds, i.e., covalent and ionic bonding. The most serious limitation of the simple chemical bond treatments on chemisorption is the negligence of the differences in the electronic states near the surface of a solid, those associated either with the solid as a whole or the isolated atoms of the solid. In the case of highly ionic bonds, some success has been obtained⁽⁴⁾ in checking experimental heats of adsorption against the values calculated using the classical electrostatic theories. Another method used to describe

surface bonding involves ligand-field theory. In this theory, the effects of a local, ordered environment in the metal on the adsorption bond are considered. These studies represent the most fundamental approach to adsorption and deal with idealized systems, often one dimensional, and employ the LCAO approximation of the molecular orbital theory. Qualitative explanations regarding adsorption are now possible, but these theories do lead to some interesting and provocative results such as general criteria for existence of bonds of surface states outside the region of normal crystal bonds.

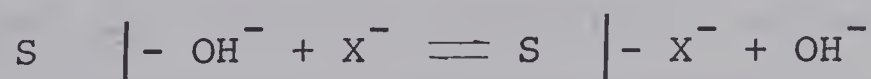
B. Collector Adsorption Theory

In flotation systems, the adsorption reactions at solid-liquid interfaces are the type that change hydrophilic solid surfaces to hydrophobic surfaces. The primary adsorbate which accomplishes this change is called a 'Collector'. The function of collectors at solid-liquid interfaces and their selective affinities for mineral surfaces are the dominant concerns in flotation studies. The action of a collector in rendering a mineral surface hydrophobic is determined by the nature of the collector used and the mineral. This action is also affected by the form of attachment of the collector on the mineral surfaces.

Solubility Theory: In early days, Taggart proposed the chemical or solubility theory of collector adsorption.⁽⁴¹⁾ Taggart postulated that flotation occurs because of metathetic reactions between the collector and the mineral surface. All interactions between flotation reagents and mineral

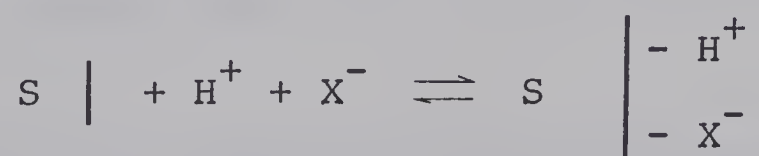
surfaces were believed to be one of the well recognized types of chemical reactions with the resulting surface compounds having the same properties as the corresponding bulk chemical compounds. In effect, this theory presumed that the mineral, or the oxidation products on the mineral surface, is more soluble than the collector salts formed as a result of the interaction between the mineral and the collector. This mechanism of adsorption has been shown to lack general validity since some collector salts are more soluble than either the mineral or oxidation products. While this mechanism completely neglects the crystal structure, surface electrical properties, and physical adsorption phenomena, nevertheless it is a useful guide in the selection of collectors and modifying agents.

Ion Exchange Theory: Proposed by Gaudin,⁽¹⁶⁾ and Sutherland and Wark,⁽⁴⁰⁾ the ion exchange theory of collector adsorption mechanism has received wider acceptance. The proponents of this theory believed that since the collector ions are generally the most predominant species in solution (this point of view has been opposed by Cook⁽⁵⁾⁽⁶⁾), these ions are adsorbed on the mineral surface by replacing previously adsorbed ions. For example, the adsorption reaction of an anionic collector ion at a mineral surface may be explained as the exchange of an collector anion for an adsorbed hydroxyl ion as illustrated below:



where S is the solid and X^- represents the collector anion. In this theory, little attention was given to the structure of the electrical double layer which surrounds mineral particles. For the sulfide and salt-type minerals, the anionic collectors such as xanthates and fatty acids are commonly used as collectors. Considering that these minerals usually have negative surface potential in a weak alkaline solution, the collector anions must diffuse against the coulombic potential barrier in the electrical double layer in order to chemisorb. This seems to be unlikely even considering that some flotation may occur with very low surface coverage of collector.

Ion-pair adsorption mechanism is also conceivable from the electrostatic consideration at the solid-liquid interface. In this case, the counter ion is also adsorbed along with the collector ion, and neutralizes the charge by following reaction:



This ion-pair adsorption mechanism can provide reasonable explanation regarding electrokinetic surface phenomena at solid-liquid interfaces.

Ion exchange and ion-pair adsorption models are shown in Fig. 2A and Fig. 2B respectively.

Hydrolytic Adsorption: In recent years, Cook et al (5) (42) proposed the hydrolytic adsorption mechanism, which is also known as the neutral collector theory. In their

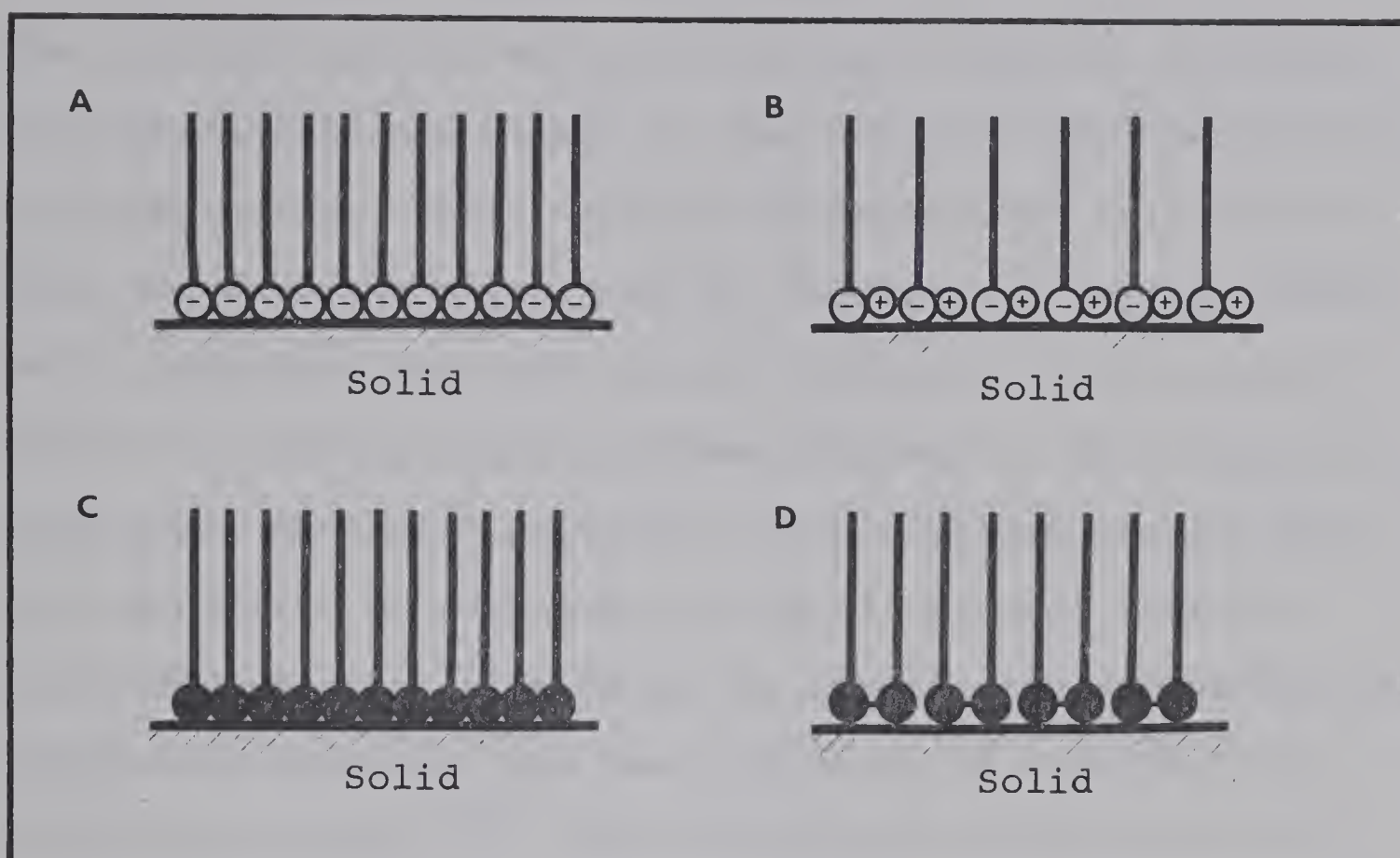


Fig. 2. Collector Adsorption Models

A: Ion-exchange B: Ion-pair Adsorption
 C: Hydrolytic Adsorption
 D: Xanthate-type Collector Adsorption

① — Ionized Collector ● — Neutral Collector
 ⊕ Counter Ion

theory, emphasis is placed on the importance of free acids and free bases as the most predominant collector. They considered the effective collector to be a non-ionic species derived from the hydrolysis of a ionized collector in a solution. Therefore, the following two reactions must take place for the hydrolytic adsorption, i.e., the hydration of collector ion followed by subsequent adsorption on the surface in molecular form:



The collector in its molecular form can approach the solid surface closely and remain on the surface independent of the surface charge. Their original arguments for this theory were based on the higher surface activity of neutral heteropolar molecules than that of the ionized molecules, as a result of electrokinetic surface phenomena. This hydrolytic adsorption mechanism provides a good explanation regarding the adsorption of xanthates on sulfide mineral surfaces. In sulfide mineral flotation, the dixanthogen (an oxidation product of xanthate) has been proven to be an effective collector species.⁽³³⁾ This dixanthogen interacts with a surface metal ion of the crystal lattice to form a metal-dixanthogen salt. The hydrolytic adsorption model and xanthate adsorption on sulfide mineral surface are visualized in Fig. 2C and Fig. 2D. Some of the experimental results, however, can not be properly explained by this theory. It was observed that by increasing the concentration of collector, the surface potential of the solid changes sign. For example, a negatively-charged quartz surface becomes positive in a cationic collector solution.⁽¹⁷⁾ This phenomenon is hardly explainable by the neutral molecule theory, even considering that a very small amount of excess ions on a solid surface can change the magnitude of the surface potential markedly.

C. Hemimicelle Hypothesis

Collectors can be adsorbed on a solid surface in many forms. In some cases, they form a complex compound and an unionized molecular film. They may also adsorb in the electrical double layer of the solid surface forming multilayers. Regardless of the kinds of species formed, the arrangements of collector species at the solid-liquid interface must be such as to provide hydrophobicity to the solid surface. The orientation of heteropolar molecules at the solid-liquid interface depends upon the collector concentration, the length of the non-polar hydrocarbon chain, and particularly on the nature of the polar head.⁽²⁵⁾ A precise explanation regarding the arrangement of collector species on a solid surface is, however, not yet available.

Gaudin and Fuerstenau investigated the mechanism of the flotation of quartz by cationic collectors.⁽¹⁷⁾ From their experimental results, they found that the collector ions show a marked affinity for the surface above a certain concentration. These investigators cited this result as evidence of the change in the structure of the adsorbed layer with hemimicelle formation. Schematic diagrams illustrating collector ion association on the solid surface and the formation of a hemimicelle are shown in Fig. 3.

At very low concentrations, the collector ions are adsorbed on the solid surface as individual ions with their non-polar hydrocarbon chains randomly oriented⁽¹⁾⁽¹⁷⁾ (see Fig. 3A). With increased collector concentration, the non-

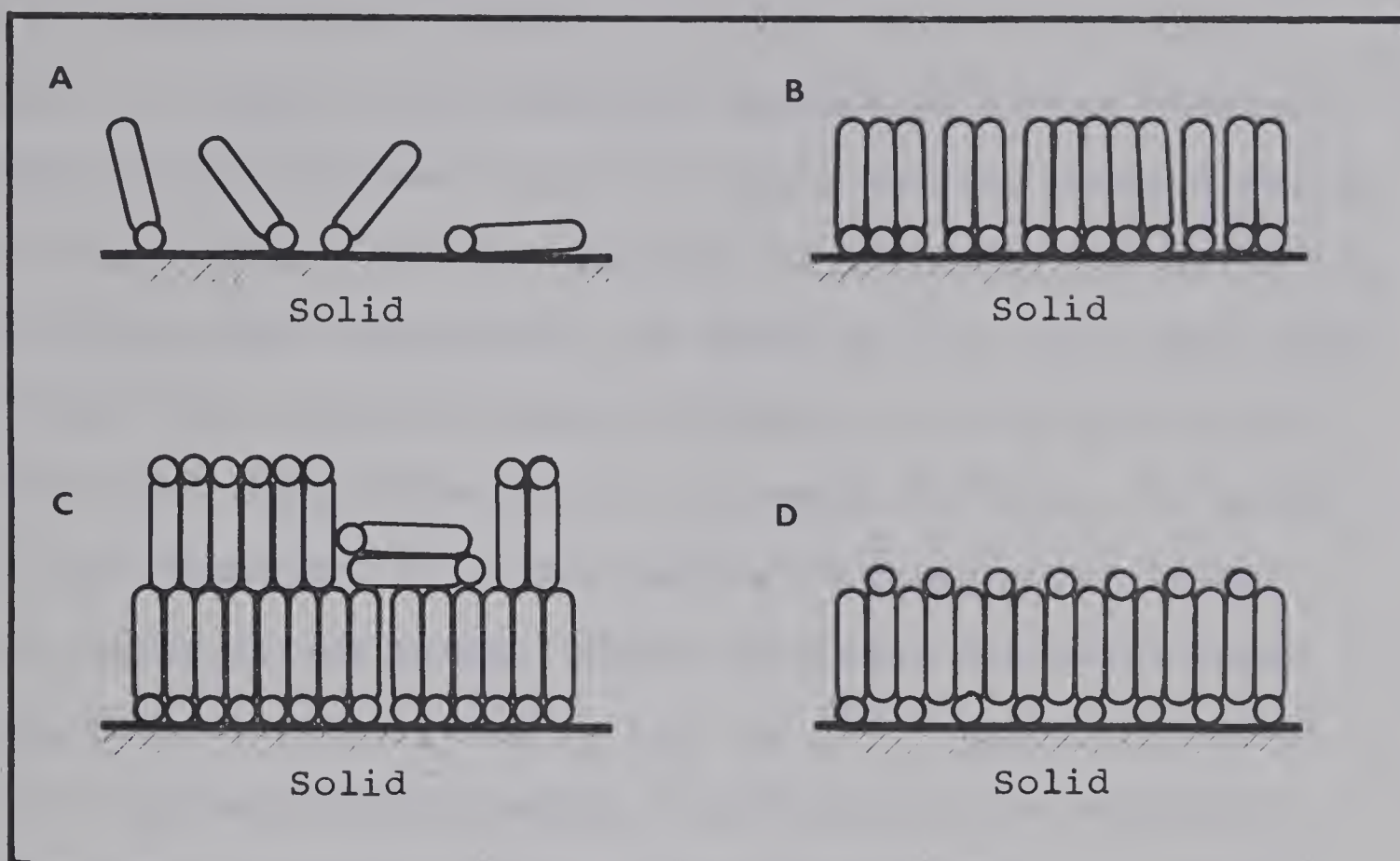


Fig. 3. Collector Ion Association on a Solid Surface
 A: Random Arrangement at Low Collector Concentration
 B: Hemimicelle
 C: Multi-layer Formation at High Collector Concentration
 D: Alternate Arrangement of Collector
 (○— Collector Ion)

polar radicals begin to attract each other more and more because of the increasing dispersion forces between the hydrocarbon chains. Increasing density of the collector on the surface leads to the orientation of the collector species at a definite angle to the solid surface. Ions associated in this way on a solid surface were named hemimicelles by Gaudin.⁽¹⁷⁾ Hemimicelle formation on the solid surface is shown in Fig. 3B. The orientation of the adsorbed collector species with their polar heads towards the solid surface and

with the hydrocarbon chains sticking out into the liquid phase, is known to be favorable because of strong electrostatic forces between the ionic heads and the charged solid surface. With a further increase in collector concentration, the multi-layer adsorption, as shown in Fig. 3C, takes place. A great deal of experimental evidence is available to confirm multi-layer formation on a mineral surface. In spite of this evidence, the exact nature of these multi-layer structures is not known. Gaudin proposed the multi-layer structure as illustrated in Fig. 3C.⁽¹⁷⁾ Gaudin's hemimicelle and multi-layer models do not seem to be valid for fatty acid-type collectors. If the electrostatic interaction is considered as a major force for collector adsorption, one can easily imagine that there will be strong repulsive forces among the adsorbed polar heads. These repulsive forces will be predominant with increasing association of the collector species on the surface. For collectors with a long hydrocarbon chain, the dispersion forces among the hydrocarbon chains are also extensive. In this case, the alternate arrangement of collector species on the surface, as shown in Fig. 3D, seems to be more probable. However, this kind of adsorption configuration, the solid surface becomes water-avid rather than the reverse. Consequently, aggregates of collector species in the surface layer must be formed without reversing their orientation or the aggregation should be favorable in providing a hydrophobic nature to the surface.

D. Adsorption Mechanisms of Fatty Acids

Most collector adsorption theories and models so far proposed by other research workers are principally based on the interactions between the collector polar head and the mineral surface. These theories maintain that the collector polar heads are held on the surface by electrostatic forces and/or covalent forces. The collecting mechanism of xanthate (for sulfide minerals) and cationic-type collectors (for silicates and oxides) are explainable using the above-mentioned theories.

The adsorption forces of xanthate on a sulfide mineral surface are proven to be covalent in nature.⁽³³⁾ The polar head of xanthate (actually dixanthogen) overlaps on the metal orbitals which appear from the crystalline solid surface. In order to obtain the most favorable overlap, the collector species are adsorbed at a definite angle, possibly perpendicular, to the surface. Therefore, the compact monolayer formation with collector polar heads sticking on the surface seems to be valid for xanthate-type collectors.

Experimental evidence has shown that the adsorption reactions of collectors on silicates and oxide minerals are electrostatic in nature. Therefore, for flotation of these kinds of minerals, close control of the surface electrical charge is very important.

The nature of collecting forces of fatty acids for salt-type minerals is inexplicable by the above theoretical

considerations. The salt-type minerals usually have a negative surface potential in the flotation circuits. Therefore, adsorption of anionic fatty acid heads on the negatively charged mineral surfaces is impossible from an electrostatic point of view. Cook⁽⁵⁾ mentioned the possibility of neutral $(RCOOH)_2$ molecular species forming and adsorbing at the solid-liquid interfaces. This neutral molecular species could then approach the surface without being repulsed by electrostatic forces. The principal forces which hold the collector heads on the surface were not mentioned in Cook's studies. In their infrared studies on adsorbed oleate on salt-type mineral surfaces, Peck and Wadsworth showed that a metal-oleate salt is formed on the surface.⁽³²⁾ The direct interactions of the oleate species with the surface metal ions in the crystalline lattice seem rather unlikely on the basis of the crystallochemical nature of a salt-type mineral surface. Most of the salt-type minerals have large anions in their crystal lattice. In a cleavage plane, the smaller metal ions are more or less sealed by the adjacent, larger anions. Therefore, the ionic head of the collector must squeeze in through the anions in order to reach to the metal cations. This reaction seems unlikely, because the collector head is usually larger than the space between the surface anions. It may, however, be possible for the oleate ions to form a metal-oleate salt with hydrated metal ions. These metal ions would be held on the surface as the counter ions making up the double layer. If this is the case, com-

compact monolayer formation is not possible because of the repulsive forces of the charged heads as explained in the previous section (Hemimicelle Hypothesis). It has been also observed that the collecting power of a collector increases with increasing the hydrocarbon chain length. Considering that the hydrocarbon chain in a collector molecule provides the hydrophobicity to the solid surface, different kinds of collectors (i.e. xanthate and fatty acid) with identical hydrocarbon chains should exhibit almost the same collecting power. This is not true. Xanthate-type collectors, with relatively short hydrocarbon chains (generally less than C-6), have excellent collecting properties for sulfide minerals. Fatty acids and cationic collectors show almost no collecting power with a hydrocarbon length less than 6. This phenomenon is inexplicable by the compact monolayer adsorption model (Fig. 3B).

The above considerations suggest a difference in collecting mechanisms among different types of collectors. For fatty acids, the possibility of direct interactions between the hydrocarbon chain and the surface has already been mentioned.⁽¹⁹⁾ However, the nature of this interaction is in doubt. Therefore, the need for direct experimental evidences to elucidate the fatty acid adsorption mechanisms on salt-type mineral surfaces is apparent.

3. Electrokinetic Phenomena at Solid-Liquid Interfaces

A. Electrical Double Layer

If two phases of different chemical constituents are

in contact, an electrical potential difference is developed between the two phases. If a solid is brought in contact with an aqueous solution, charged species are redistributed across the interface, forming an electrical double layer. For the formation of the electrical double layer, the solid surface should be charged. Three possible mechanisms by which this potential is developed on the solid-liquid interface can be imagined: ⁽³⁵⁾

(a) The crystal lattice of the solid may contain a net positive or negative charge arising from defects or lattice substitutions; the net charge is therefore compensated by an equivalent ionic charge at the surface. In contact with water, the compensating ions dissociate to form the counter ions of the double layer.

(b) In the case of sparingly soluble ionic solids, an equilibrium exists between the ions making up the surface of the crystal and these same constituent ions in the solution. The concentration of these ions is determined by the solubility product of the solid material. Thus, an excess of the positive constituent ions in the solution makes the solid surface become more positive; an addition of the excess negative constituent ions makes the surface more negative.

(c) This mechanism includes the adsorption of specific ions from the solution. Specific ions may

be strongly adsorbed, or chemisorbed by the formation of surface complexes, or compounds.⁽²⁹⁾ Adsorption may also be aided by hydrogen bond formation or by the London dispersion (van der Waals) forces, particularly with large organic molecules or ions.

The interaction energy of water with different ions occurring in the solid surface also varies widely. For this reason, some ions are transferred into the solution in greater amounts than the others. The preponderant transfer of an ion into solution causes a disturbance in the electrical equilibrium on the solid surface. As a result, the surface becomes electrically charged. The surface potential of a solid depends very much on the concentration of those ions which serve as the building blocks of the solid.⁽¹²⁾ These constituent ions, together with other ions which directly influence the concentration of the constituent ions, are called Potential Determining Ions. As the concentration of one potential determining ion increases, it becomes more and more difficult for this ion to escape from the solid surface. Above a certain concentration, these ions start to be adsorbed on the solid surface from the solution. Therefore, there will be a point where plus and minus charges are exactly balanced at the solid surface and the surface potential is zero. This concentration is called the Isoelectric Point or Zero Point of Charge (zpc).

The charge on the surface of a solid will tend to attract ions of opposite sign from the solution to the

vicinity of the solid. These ions form an ordered layer which is bonded to the surface such that this layer moves together with the solid body. Next to the ordered layer of ions is a diffuse layer which decreases in concentration with increasing distance from the solid. The ions in this diffuse layer can be separated from the solid as the particle moves through the solution. During the departure of the ions of the diffuse layer away from the surface, the electro-neutrality of the system is disrupted and a difference in the potential arises between the moving particle and the liquid. This potential is called the Electrokinetic or Zeta Potential (ζ).

The schematic diagram of the electrical double layer developed around a solid particle in an aqueous solution is shown in Fig. 4.⁽³⁴⁾

The solid particle is surrounded by a layer of anchored oppositely charged ions followed by the aqueous layer containing the diffused counter ions and bulk liquid. The thickness of the diffuse layer, together with the zeta potential, is greatly affected by the concentration and the valency of the counter ions in the solution.⁽³⁵⁾ The effect of the electrolyte concentration and valency on the value of the electric potential (ψ) as a function of distance from the surface is shown in Fig. 5. Fig. 5A shows the effect of mono-valent electrolyte concentration for an arbitrary

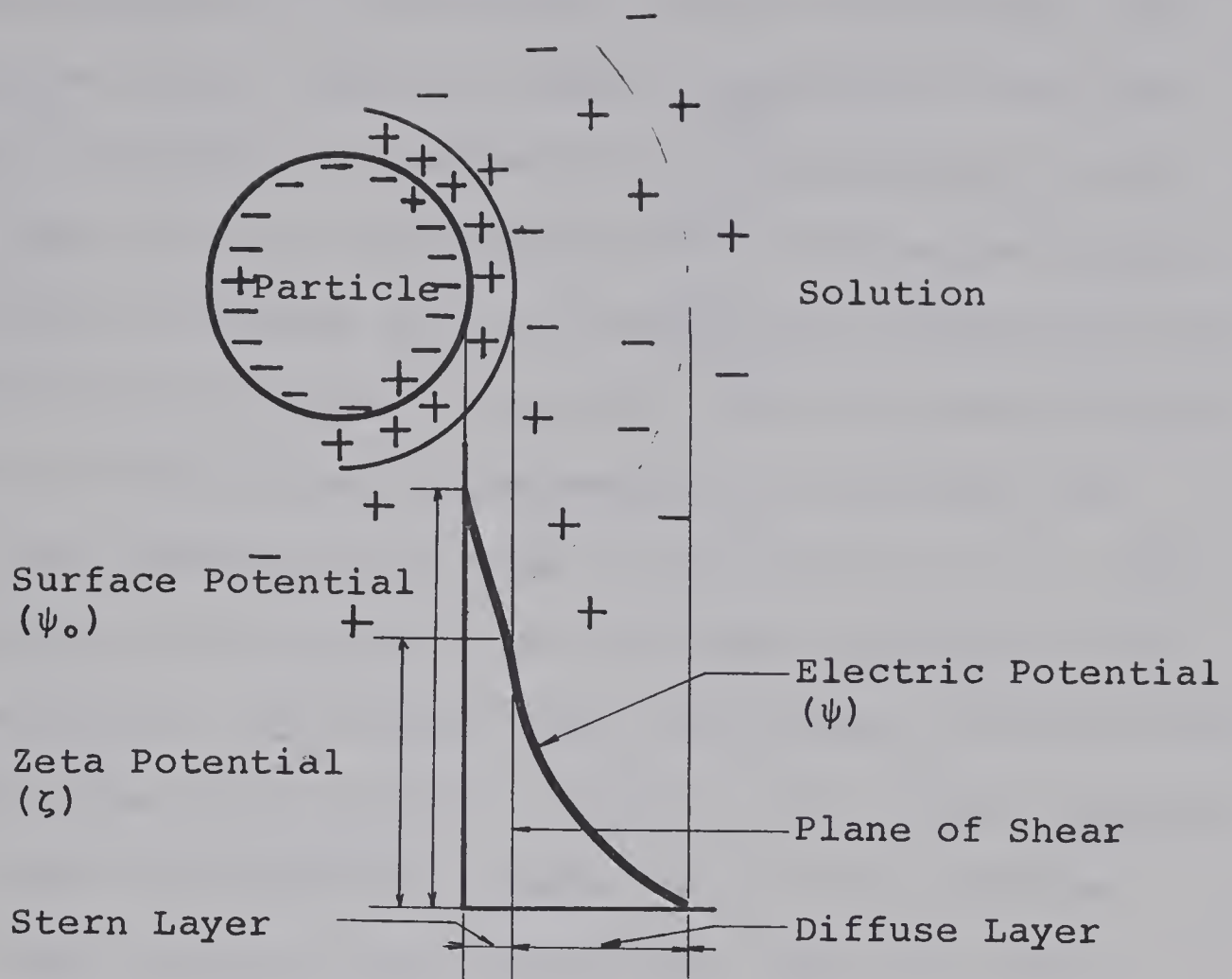


Fig. 4. Electrical Double Layer Around A Solid Particle

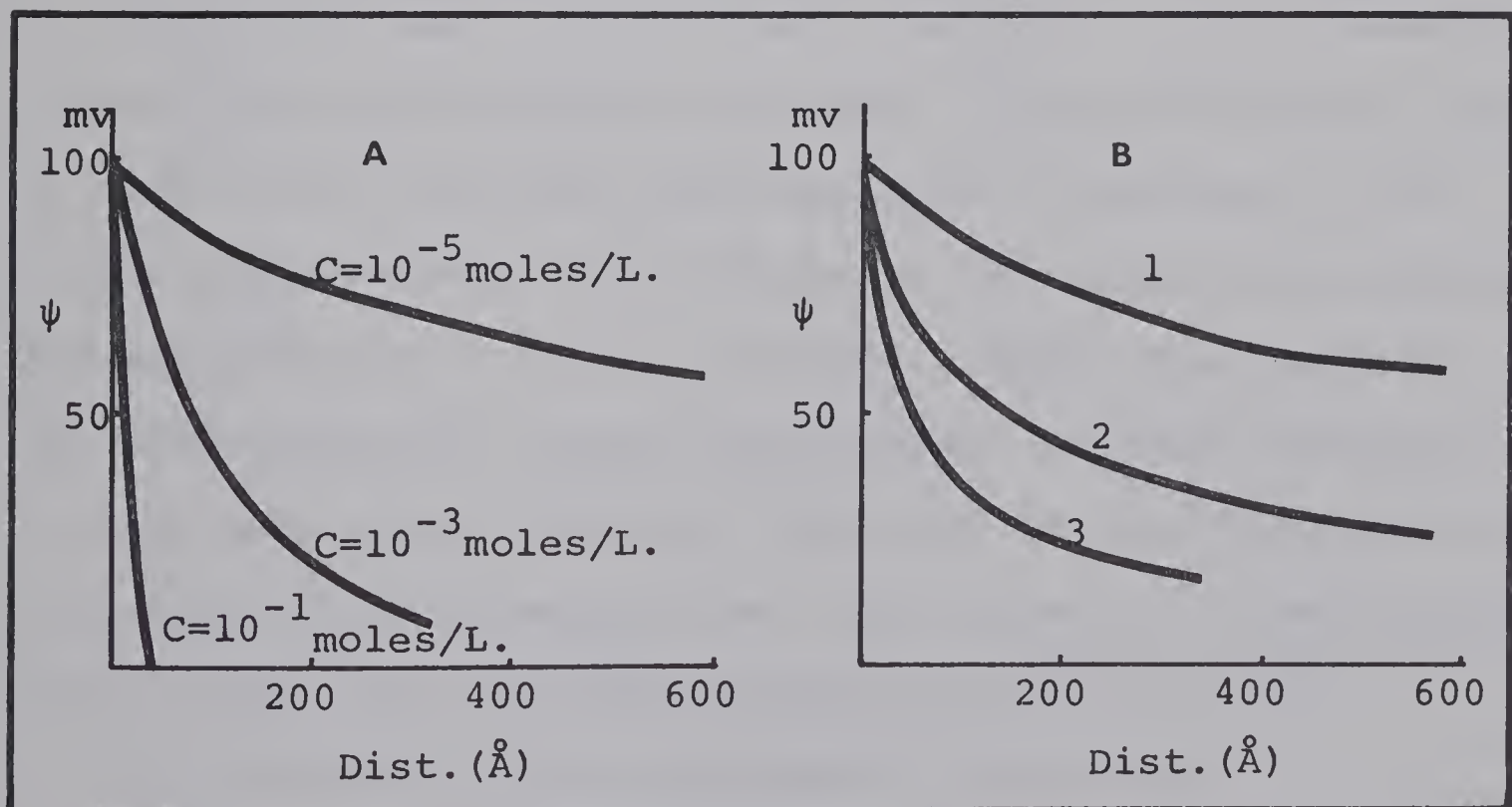


Fig. 5. The Effect of the Electrolyte Concentration and Valency on the Electric Potential (ψ)
 A: Effect of Monovalent Electrolyte Concentration
 B: Effect of Counter Ion Valency (10^{-5} Mole/L.)

surface potential (ψ_0) of 100 mv. Added electrolyte compresses the double layer, so that it approaches zero more rapidly; the degree of compression is proportional to the square root of ionic concentration.⁽²¹⁾ The marked effect of counter ion valency with an electrolyte concentration of 10^{-5} mole/litre is shown in Fig. 5B. The thickness of the electrical double layer is decreased by increasing the valency and decreasing the size of the counter ions. This phenomenon can be explained by the closer approach to the solid surface by the smaller ions, and higher neutralization power for ions with a higher valency. This higher neutralization power will provide a sudden drop of the diffuse double layer potential and accordingly lower the zeta potential.

The zeta potential of a system is usually determined by one of the basic electrokinetic methods. In the electrophoresis and electroosmosis methods, a known electrical field is set up, and the resulting mechanical properties of the system are measured. The reverse is the case in the streaming and sedimentation potential methods. Among these methods, the electrophoretic method has received the most attention. In this method, the mobility (velocity) of the particle in a potential field is measured and then converted to zeta potential by the well known Smoluchowski equation.^{(16) (35)}

B. Structure of the Electrical Double Layer

The original theoretical analysis regarding the structure of the electrical double layer was carried out by

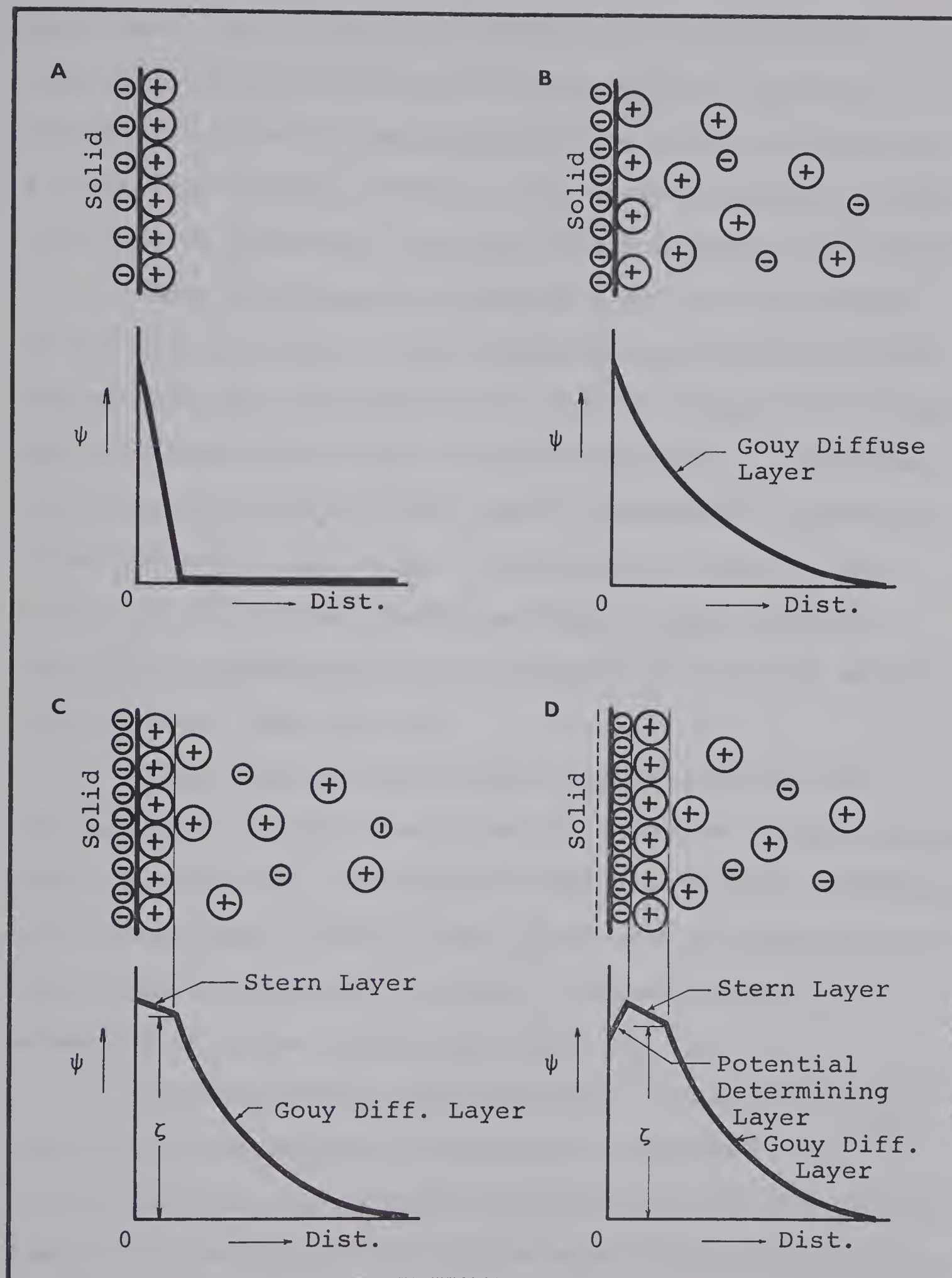


Fig. 6. Potential Variation in Different Electrical Double Layer Structures

Helmholtz. He originally proposed that the potential difference between two phases resides in two layers of charges - a layer of positive ions immediately adjacent to a negatively charged surface. This theory predicts a linear variation in potential across the phase boundary (see Fig.6A).

Gouy and Chapman recognized that the like charges on the solution side of the interface would attract unlike charges causing a disturbance or diffuse charge distribution. Their diffuse double layer structure predicts a non-linear potential distribution which can be calculated, assuming a Maxwell-Boltzman type charge distribution. The Gouy and Chapman theory of the electrical double layer, however, predicts a fantastically high concentration of ions near the solid surface (see Fig. 6B).

Stern recognized that the counter ions can not approach the surface closer than the distance of the hydrated radius of the ions. He believed that the specific adsorption of ions and their finite sizes could lead to formation of an inner compact layer of ions with a second diffuse layer extending into the liquid phase (see Fig. 6C).

Grahame further improved Stern's treatment by also considering the degree of solvation of adsorbed ions.⁽³³⁾ In his analysis, he included the fact that both anions and cations can be adsorbed by forces other than electrostatic, i.e., chemical or van der Waals. Grahame postulated that the non-electrical forces are chiefly operative for anions, which become adsorbed with loss of their hydration shells.

On this basis, there is reason for further dividing the double layer into three parts: (1) a layer of unsolvated potential determining ions (usually anions) in the solid surface. (2) a layer of tightly held, hydrated counter ions (specifically adsorbed). (3) an outer diffuse layer extending into the solution (Fig. 6D). According to this model, the surface potential can be drastically changed, and even reversed in sign, by a change in concentration of the potential-determining ion. The effect of a change in the Stern layer and Gouy diffuse layer will be to reduce the potential toward zero.

C. Significance of Surface Potential in Flotation

Considerable attention has been directed toward the electrokinetic phenomena of mineral particles for the purpose of characterizing mineral surfaces and collection mechanisms in a flotation system.

Fuerstenau and Modi⁽¹³⁾ first stressed the importance of determining the sign of the surface charge of oxides in order to ascertain whether a mineral would respond to flotation with an anionic or cationic collector. Iwasaki and Choi⁽²²⁾ studied the electrokinetic and flotation behavior of geothite and hematite using different kinds of collectors. In their experiments, they showed that the cationic collectors are effective when the mineral surface is negatively charged and conversely anionic collectors are effective for positively charged surfaces. At the zpc of a mineral, flotation recovery is reduced when using either the anionic or

cationic collectors. Smolik et al⁽³⁷⁾ also compared pH vs. recovery curves with pH vs. zeta potential curves for various silicate minerals using dodecylamine acetate (cationic) and sodium dodecyl sulfonate (anionic) as collectors. From their experimental results, Smolik arrived at the same conclusion as Iwasaki did. Furthermore, Smolik concluded that the collectors are in ionic form, and are held by the electrostatic forces in the double layer.

The concept that the collectors are in ionic form at the solid-liquid interface has been strongly opposed by Cook.⁽⁵⁾ He proposed that in a flotation system with zeta potential ranging between 20 to 50 millivolts and with total ionic strength about 10^{-4} to 10^{-5} mole/litre, the net electrokinetic charge (sum of the positive and negative charges) seldom exceeds more than 0.1 percent of the total charges that appear at most solid-liquid interfaces. From the above reason, Cook concluded that unless one takes into account the counter ion adsorption, or ion exchange, simple ion-collector adsorption would charge the solid surface by impossible magnitudes. On the other hand, the pH vs. zeta potential curves seem to be meaningless in either ion-exchange or ion-pair adsorption mechanisms.

It is obvious that the surface charge of a mineral has pronounced effects on the collector ion adsorption. If the adsorbing species are neutral, dipolar-type molecules, the potential barrier in an electrical double layer may be significantly lowered and adsorption is not greatly affected

by the surface potential of a solid. Physical forces such as electrostatic and van der Waals forces, seem to play a significant role for the collector adsorption on the silicates and oxides. Therefore, the surface potential of a solid is very important for this kind of mineral flotation. The surface potential does not seem to have a pronounced effect on the flotation of sulfide and salt-type minerals. With these minerals, it is believed that the collector species are held on the mineral surfaces by chemisorption.⁽¹²⁾

EXPERIMENTAL METHODS

1. Materials

A. Reagents

Fatty acids used for all the flotation tests were converted before use to their corresponding sodium soaps. These soaps were prepared by reacting the fatty acids with 150 percent of the stoichiometrically required amount of 0.1 N sodium hydroxide.

Fatty acids used in the experiments are listed below:

N-caproic Acid $\text{CH}_3(\text{CH}_2)_4\text{COOH}$	95% Pur. (Mat.Co.)
N-caprylic Acid $\text{CH}_3(\text{CH}_2)_6\text{COOH}$	" " (K&K Co.)
Decanoic Acid $\text{CH}_3(\text{CH}_2)_8\text{COOH}$	" " (")
Lauric Acid $\text{CH}_3(\text{CH}_2)_{10}\text{COOH}$	" " (")
Myristic Acid $\text{CH}_3(\text{CH}_2)_{12}\text{COOH}$	" " (E.M.Co.)
Palmitic Acid $\text{CH}_3(\text{CH}_2)_{14}\text{COOH}$	" " (")
Stearic Acid $\text{CH}_3(\text{CH}_2)_{16}\text{COOH}$	" " (Fis.Co.)
Oleic Acid $\text{CH}_3(\text{CH}_2)_7\text{CH}=\text{CH}(\text{CH}_2)_7\text{COOH}$ (cis.)	" " (")
Linoleic Acid $\text{CH}_3(\text{CH}_2)_4\text{CH}=\text{CHCH}_2\text{CH}=\text{CH}(\text{CH}_2)_7\text{COOH}$	97 " (K&K Co.)
Linolenic Acid $\text{CH}_3\text{CH}_2\text{CH}=\text{CHCH}_2\text{CH}=\text{CHCH}_2\text{CH}=\text{CH}(\text{CH}_2)_7\text{COOH}$	99 " (")

The pH adjustments were made using ACS grade of HCl and NaOH. Other chemical reagents used for these experiments also met the ACS specification.

Demineralized-distilled water (DD water) containing less than 0.3 ppm. dissolved salts (expressed as NaCl), was used for all test solutions.

B. Sample

Massive and well-crystallized natural barite was supplied by J. Foster Irwin Engineering Company of Edmonton. This material was from the Barite Mountain Deposit located near Ross River, Yukon. Pure barite was hand picked from the original sample and washed thoroughly with DD water to remove any clay and organic materials from the barite surfaces. This barite was then crushed using a laboratory jaw crusher and cone crusher. From the minus 4 to plus 8 mesh fraction, only very pure and well-crystallized barite particles were again hand picked. This pure barite was further wet-ground using a laboratory stainless steel rod mill. This pure barite slurry was wet-screened and the minus 100 plus 200 mesh size fraction was taken and dried for experimental use. This barite sample (-100 +200 mesh size) was then passed through an Induced Roll Magnetic Separator (Carpco Mfg. Inc.) three times to ensure removal of any iron-bearing impurities introduced during the grinding stage. Chemical analysis of this sample showed more than 99.6 percent purity as BaSO_4 , and no impurities were detected by X-ray diffraction examination. A portion of this sample was

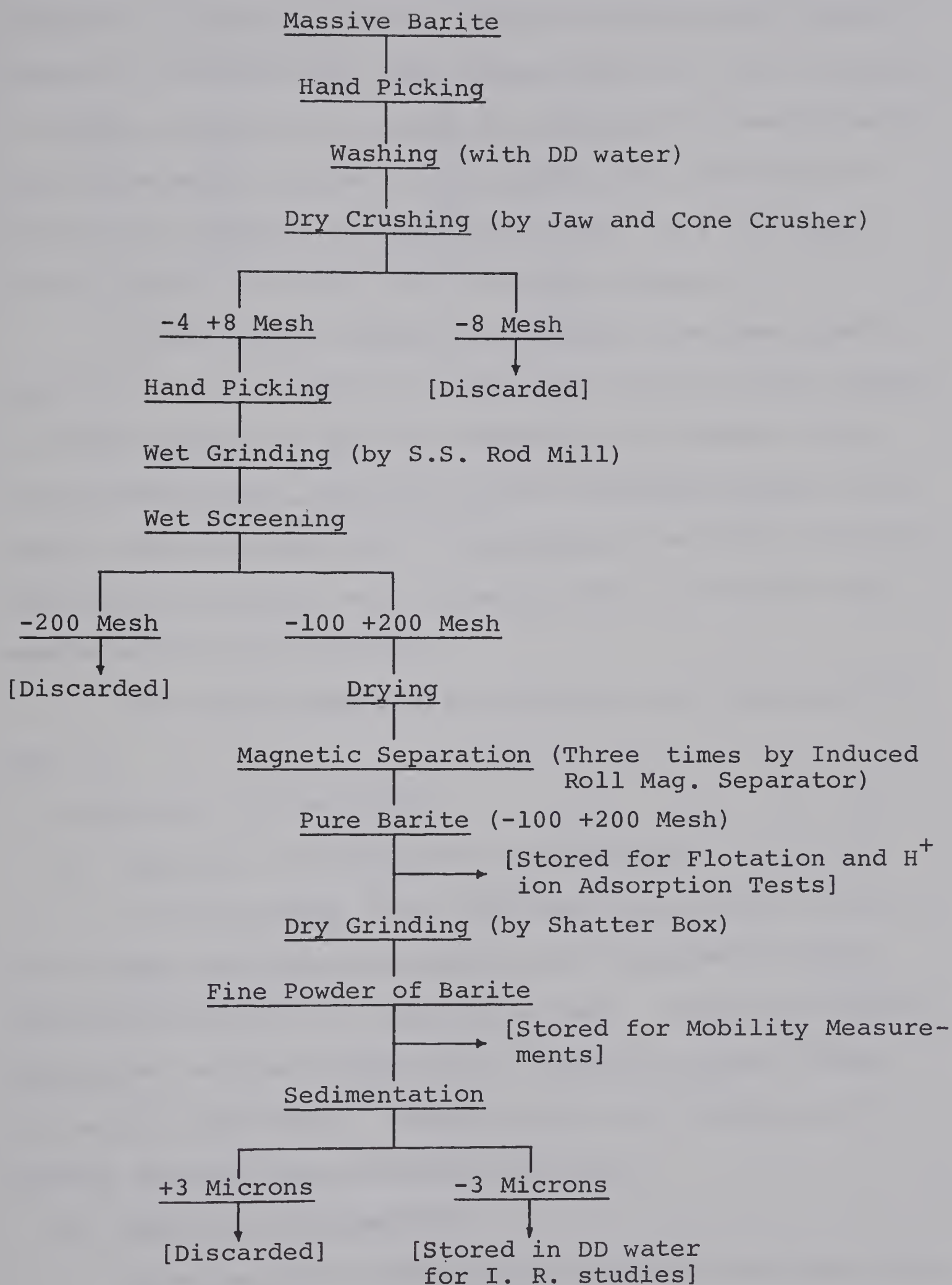


Fig. 7. Sample Preparation Procedures

stored for flotation testing, and the remainder was further ground by a Shatter Box (Spex Industries Inc.) for 15 minutes to obtain material fine enough for the mobility measurements. From the material ground in the Shatter Box, the minus 3-micron size sample was stored in DD water as a 70 weight percent slurry for use in the infrared studies.

A pure quartz sample was prepared from pure quartz crystals in a way similar to that used for the barite sample. To ensure removal of any iron particles introduced during the grinding stage, the material was processed using a hand magnet, then leached with 1 N hydrochloric acid for 48 hours, and washed thoroughly with DD water until no chloride ions were detected in the solution.

The sample preparation procedures are summarized in Fig. 7.

2. Apparatus and Procedures

A. Hydrogen Ion Adsorption Measurements

A 30-gm sample (-100 +200 mesh) was placed in 250 ml of DD water previously adjusted to the required pH level (initial pH levels of 3 and 9 were used). This solid-liquid mixture was stirred gently with a magnetic stirrer during the entire experiment. Changes in pH were followed with a Beckman Expanded Scale Zeromatic pH meter.

B. Mobility Measurements

Electrokinetic mobility measurements were made using a flat-type, horizontal microphoretic cell, constructed from acrylic plastic (Lucite). This cell, which was built by the

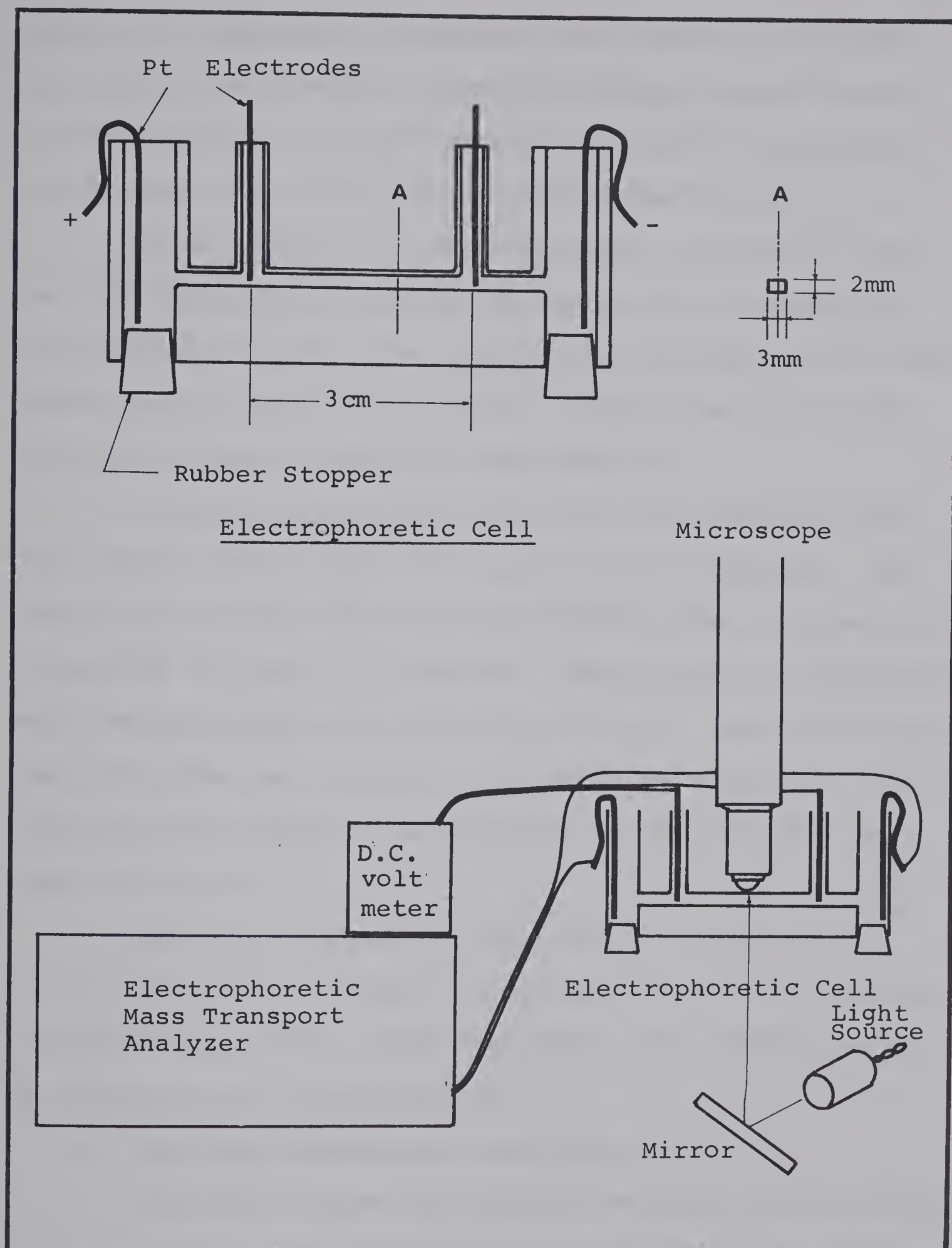


Fig. 8. Apparatus for Electrophoretic Measurement

author, was designed to eliminate the effects of electrode polarization to provide a constant voltage gradient during the measurements. The design also eliminated the effects of hydrodynamic flow during the mobility measurements.

An Electrophoretic Mass-Transport Analyzer⁽²⁷⁾ was used for supplying a constant direct current through the electrophoretic cell. The current flow through the cell was controlled to maintain a constant voltage gradient of 10 volts/cm during the mobility measurements.

A conventional microscope with X100 magnification was used to observe the moving particles in the cell. The mobility data were taken by measuring the time required for a particle to travel 150 microns. Approximately 20 measurements were made and averaged for each test. The polarity of the electrodes was changed on alternate measurements. Cell dimensions and schematic arrangement of the apparatus is shown in Fig. 8.

Mobility measurements were made in solutions of varying pH levels, barium ion concentrations, and collector concentrations. Each sample suspension was conditioned for 20 minutes before being measured.

C. Infrared Transmission Techniques

Infrared studies for adsorbed collector species were conducted by transmission of the infrared beam through a finely divided pellet sample of the adsorbent. Substrate particles were smaller than 3 microns to limit adsorption and dispersion losses of the radiation while simultaneously

providing a high surface area for adsorption.⁽⁸⁾ A vacuum die with KBr as the matrix was used to make the pellets. The procedure used is described elsewhere.⁽¹¹⁾

ACS grade of KBr was heated in a vacuum furnace at 110°C for 48 hours, and then was ground in the Shatter Box for 20 minutes. This finely ground KBr powder was again heated at 110°C overnight and stored in a dessicator. Approximately 1 ml of pure barite slurry (-3 microns size) was pipetted into 200 ml of collector solution of known concentration and pH. This collector-barite slurry was agitated with a magnetic stirrer for 20 minutes and filtered. In most of the cases, the barite particles were flocculated which made the solution easy to filter using ordinary filter paper (Whatman Filterpaper No.2 was used). The filtered solids were washed 5 times with DD water which had been adjusted to the same pH as the filtrate. This sample was dried at room temperature in a vacuum furnace and stored in a dessicator.

The sample containing the adsorbed collector was combined with ground KBr in a 1 to 50 ratio. To ensure adequate mixing, this material was agitated in a Spex Mixer for 10 minutes. It was found that a uniform distribution of sample in the KBr matrix was obtained within this mixing time. From this mixed sample, a carefully weighed 0.5 gm aliquot sample was taken for pressing. The use of an initial 10-gm charge materially minimized the weighing and mixing errors.

The 0.5 gms of aliquot sample was transferred into the 1 1/4 inch diameter die chamber and a force of 20 tons was applied to the disc for 15 minutes. The resulting sample disc was brittle, thin, and transparent. Extreme care was necessary in removing the disc from the die chamber. In each case, the infrared spectrum of the sample disc was taken immediately after it was formed. A Perkin Elmer 221G double-beam spectrophotometer was used for obtaining the infrared spectra.

The infrared spectra of pure fatty acids in liquid state were recorded directly using Irtran-2 (Barnes Engineering Co.) as a window material.

D. Modified Hallimond Tube Tests

All the flotation experiments were conducted at room temperature using a modified Hallimond Tube apparatus.⁽¹⁴⁾ The flotation tests were carried out as follows:

- (a) Two grams of pure barite sample (-100 +200 mesh) was placed in a 200 ml volumetric flask and filled with the collector solution.
- (b) The slurry was conditioned in the flask for 20 minutes, and then transferred to the Hallimond Tube.
- (c) Purified nitrogen gas was passed through the cell while constant stirring was provided by a magnetic stirrer. The float product was collected for 2 minutes. The flow of nitrogen gas and stirring speed were kept constant for all the experiments.

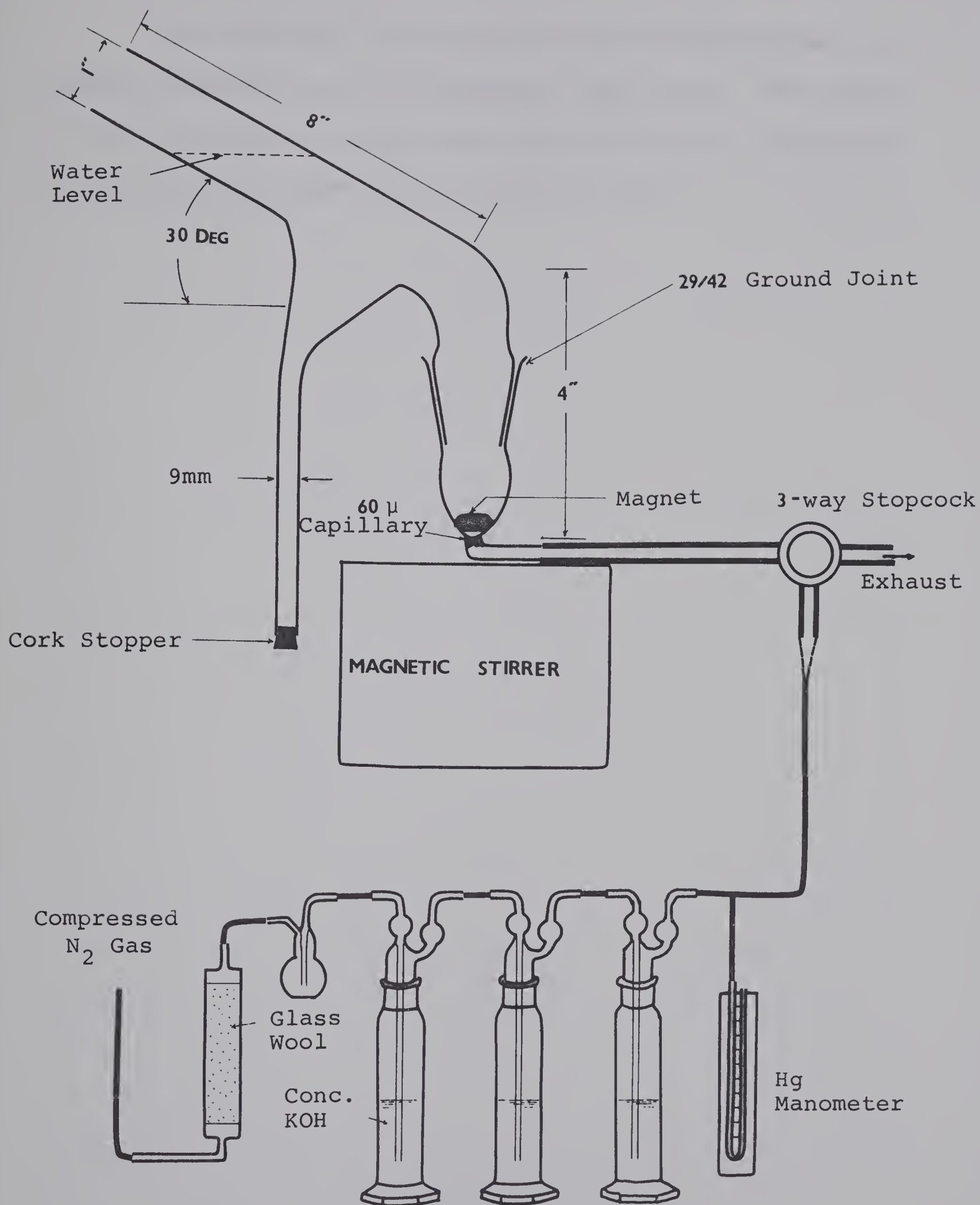


Fig. 9. Flotation Apparatus

The flotation recovery of barite was determined for various concentrations of different fatty acids. The effect of pH on flotation recovery was also determined. A diagram of the flotation apparatus is shown in Fig. 9.

EXPERIMENTAL RESULTS AND DISCUSSION

1. Electrokinetic Surface Phenomena

To study the reaction occurring at the solid-liquid interface in detail, a series of zeta potential measurements was performed for barite and quartz. From the electrophoretic mobility data (data are presented in Appendix A), zeta potential were calculated using the Smoluchowski's equation:

$$v_e = \frac{\zeta \cdot D \cdot E}{4 \pi \eta}$$

where v_e is the electrophoretic mobility, D the dielectric constant, and η the absolute viscosity of the medium. Conditions for the application of Smoluchowski's equation, in electrophoresis, are that the double layer be thin compared to the particle size and that the surface conductance be so small that the externally applied potential field is not disturbed. Since the diameters (d) of the solid particles under observation were larger than 1 micron, and the double layer thickness (τ) seldom exceeds 10^{-2} microns, the ratio of particle diameter to double layer thickness (d/τ) will be greater than 100. Therefore, the use of Smoluchowski's equation is justified.⁽³⁵⁾ Correction for the relaxation effect, originating from the surface conductance, may not be necessary, since the effects become insignificant for very large values of d/τ .⁽³⁵⁾ Bulk values of D and η can also be used in our experimental conditions without introducing significant errors.⁽²⁶⁾⁽²⁸⁾ The derivation of Smoluchowski's equation, together with its limitation for practical systems,

is explained in detail in Appendix B.

A. Variation of Zeta Potential as a Function of pH

In flotation systems the hydrogen ion plays a very important role in determining the hydration and the electrokinetic properties of a solid surface. The hydrogen ion can also control the degree of dissociation of the collector molecules, change the ionic composition of the solution, and even interact with the collector species directly.

Fig. 10 shows the variation of zeta potential of barite and quartz as a function of pH. It can be seen that the zpc of the barite is at a pH of about 4.5. The zeta potential of quartz, on the other hand, is negative over the pH range investigated, and decreased towards zero with high hydrogen ion concentration.

The potential determining role of the H^+ ion for quartz has been explained by Gaudin and Fuerstenau.⁽¹⁷⁾ The structure of quartz is believed to be an infinite, three-dimensional arrangement of tetrahedron-shaped, SiO_4^{4-} complex anions.⁽⁹⁾ A large number of polar sites are produced on the surface upon the fracture of Si-O bonds. When a crushed quartz particle is immersed in water, the surface becomes negatively charged by the reaction of the exposed polar sites with H^+ and OH^- ions followed by the ionization of H^+ ions from the surface silicic acids. The mechanism for the origin of the electrical charge of quartz in aqueous solution is shown as follows:

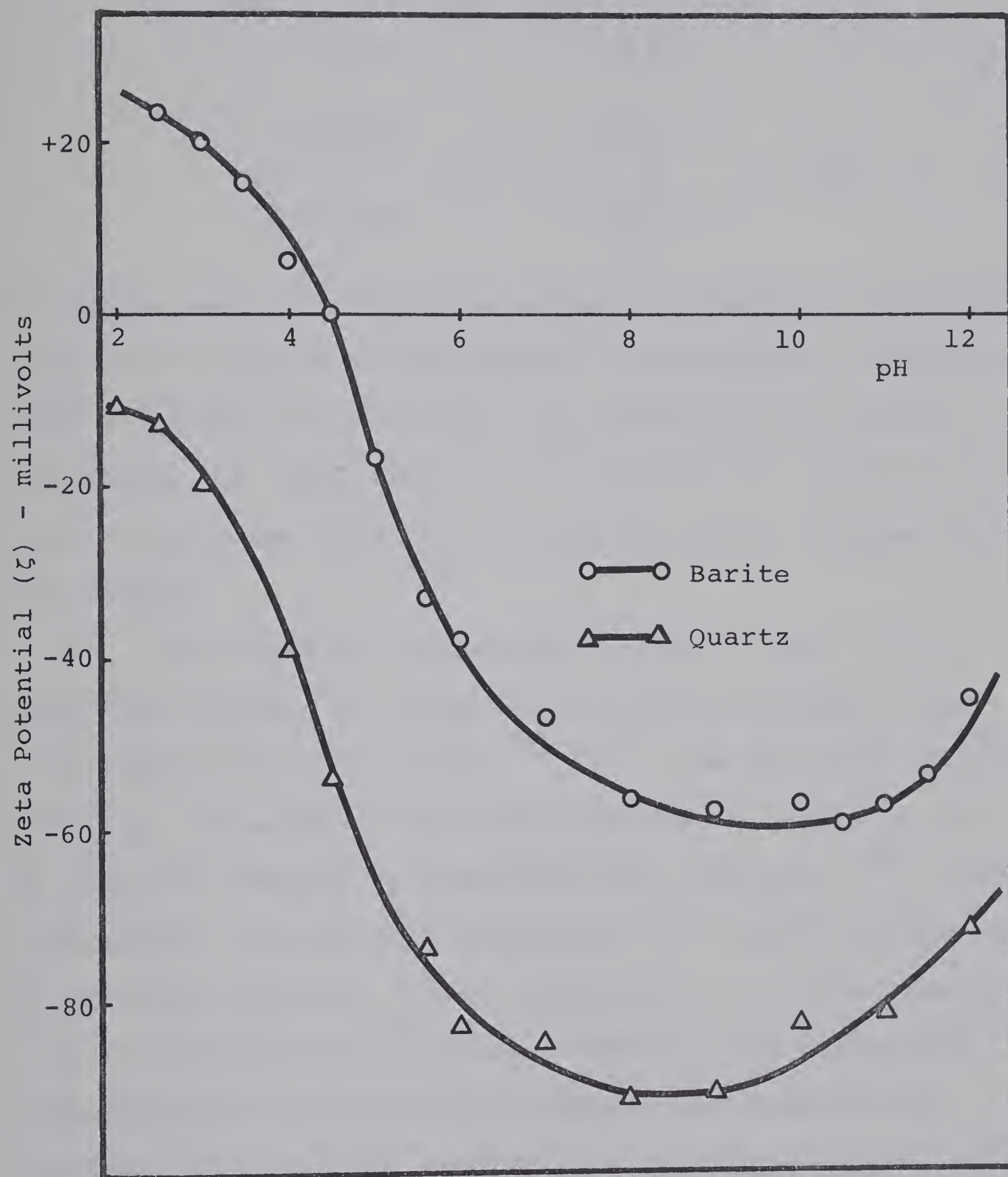
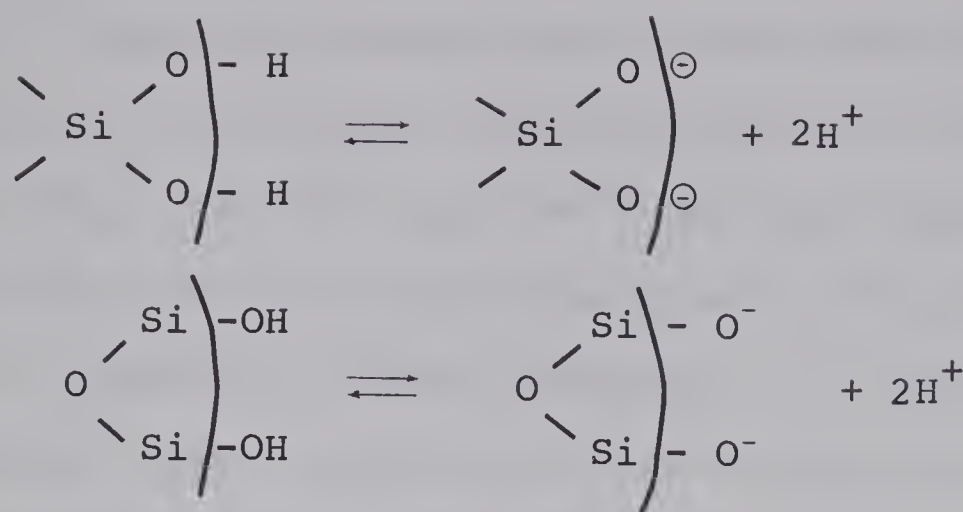


Fig. 10. Variation of Zeta Potential of Barite and Quartz as a Function of pH



As can be seen from the above schematic diagram, the surface potential of quartz is determined by the degree of dissociation of surface silicic acid. If the pH of the solution is increased, the dissociation of H^{+} ion from the surface will also be increased thus providing more negative charges on the surface.

The potential-determining role of H^{+} ion for the salt-type minerals is inexplicable by the classical potential-determining ion concept.⁽¹²⁾⁽¹⁶⁾ The variation of zeta potential for several salt-type minerals as a function of pH has been measured by Fuerstenau and Gutierrez.⁽¹⁵⁾ Their experimental results also showed that the surface potential of salt-type minerals varies considerably, and even changes sign in different pH solutions. However, the theoretical considerations regarding the electrostatic interactions between H^{+} ions and the surface of a salt-type mineral have not been made.

Experimental results in Fig. 10 show that the zeta potential of barite is negative above a pH of 4.5, and positively charged when the pH is lower than 4.5. When barite particles are immersed in an aqueous solution, some of the

Ba^{++} and SO_4^{--} ions are hydrated and go into the solution phase. Because of the higher hydration energy of the Ba^{++} ion than the SO_4^{--} ion, ⁽²⁵⁾ more Ba^{++} ions are transferred into the solution leaving behind electrons on the surface, resulting in a negative surface potential. In this way, the barite particles have a negative surface charge in a neutral solution. With increasing ionic concentration, the surface potential of a solid should be reduced to zero if one considers only electrostatic interaction between the surface and the ions in solution. ⁽³⁵⁾ The variation of the surface potential as a function of the concentration of a particular ion, therefore, immediately suggests some kind of special forces exist between a solid and certain ions. These forces are stronger than the electrostatic forces and are able to interact over the potential barrier of the surface electrical double layer. There are two possible mechanisms which can be used to explain why the surface potential of barite changes from negative to positive with increasing H^+ ion concentration:

- (a) The Debye-Hückel limiting law suggests that the presence of a large amount of inert electrolyte exerts an appreciable influence (salt effect) on the degree of dissociation of a slightly soluble salt. The salt effect is large with a high electrolyte concentration. The hydration energy for an ion of a crystal lattice can also be varied by the presence of a specific ion in the liquid phase. If a barite

surface is in contact with an acid solution, the H^+ ion will accumulate on the surface more than the other ions because of its small size and higher ionic activity.⁽³⁾ In this case, it would be easier for the SO_4^{--} ions to leave their crystal lattice than the Ba^{++} ions. Therefore, more Ba^{++} ions would be concentrated on the surface than the SO_4^{--} ions, providing a positive surface potential.

(b) An alternate explanation regarding this kind of surface adsorption phenomenon can be made by employing the ligand-field treatment of atomic orbital theory. It is observed that the bond strength in the surface layer is about 13 percent or more greater than the strength inside the crystal.⁽¹²⁾ In other words, the free surfaces will tend to adsorb appropriate ions or molecules from the solution in order to be in lower energy states. For this kind of reaction, the adsorbate approaches the surface and overlaps with the atomic orbitals which may appear from the solid surface. The overlapping of atomic orbitals will be favorable for the ions of small size because of their close approach to the surface. This overlapping is not favorable for ions with an inert gas type of electronic configuration because of their stable and high sealing effects. When barite is immersed in acidified water, some of the H^+ ions will overlap the SO_4^{--} ions on the surface.

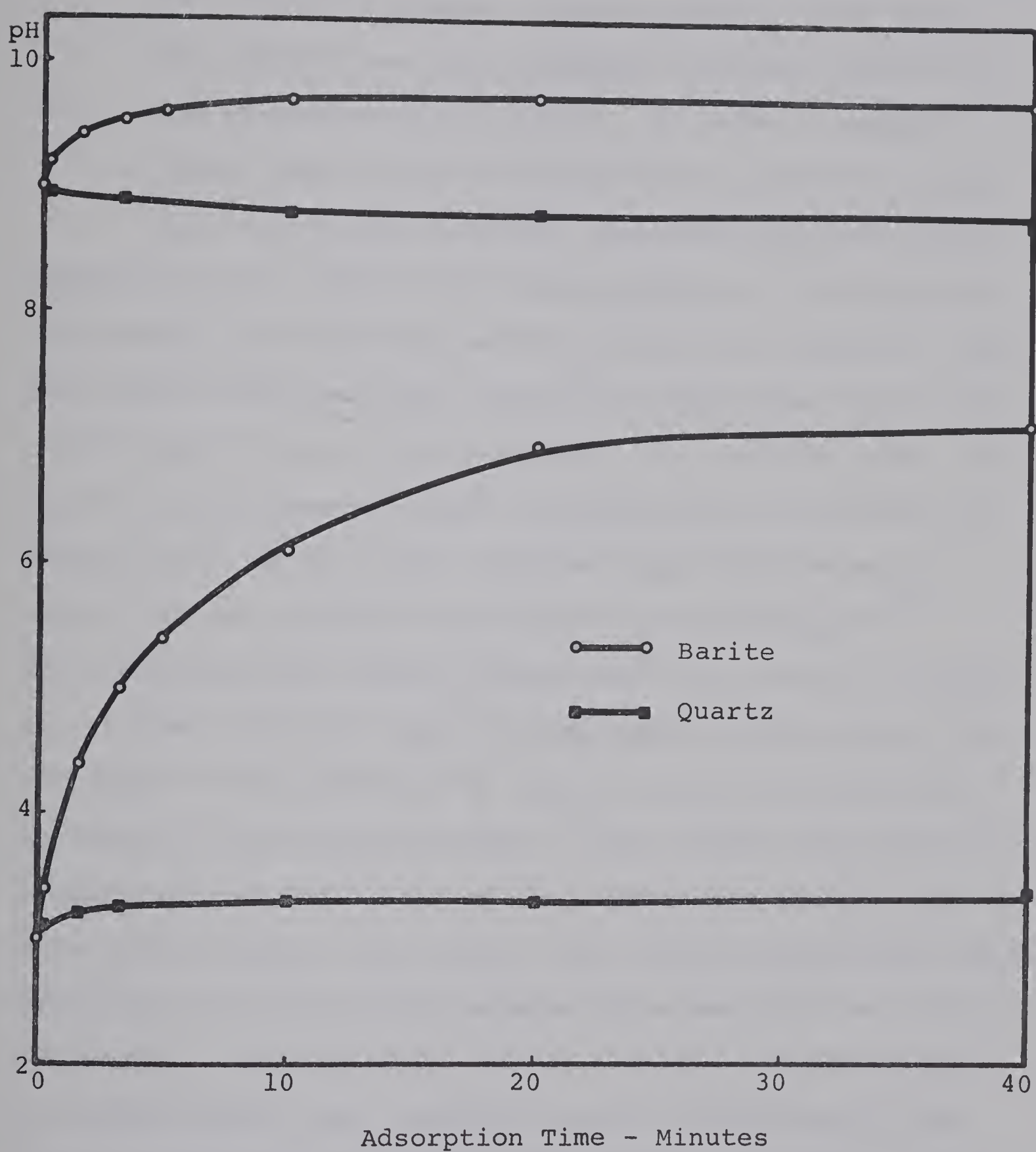


Fig. 11. Hydrogen Ion Adsorption on Barite and Quartz

With increasing H^+ ion concentration, more and more H^+ ions are adsorbed on the barite surface resulting in a positive charge. The overlapping of H^+ ions can proceed over the coulombic potential barrier of the electrical double layer, and above a certain point, the barite surface obtains a positive charge.

Fig. 11 provides evidence regarding the preferential adsorption of H^+ ions on the barite surface. The experimental results indicate that barite surface will adsorb H^+ ions even from a solution with a pH of 9.0 (where the ratio of H^+ to OH^- ions is one to ten thousand). On the other hand, the quartz surface does not show any appreciable attraction for either the H^+ or OH^- ions. Similar experiments were conducted for the silicate minerals by Deju and Bhappu.⁽⁷⁾ Their experimental results showed that the reactions between the silicate minerals and acidified water involve mainly an exchange of metal ions for H^+ ions, leading to an increase in the pH of the solution phase. They assumed the hydrolysis between exposed metal ions of the crystalline lattice may take place, and for this reason, the crystal surface may gain additional H^+ ions and the aqueous phase may acquire further alkalinity. The mechanisms of ion exchange and hydrolysis of surface metal ions, however, can not fully explain the specific adsorption nature of H^+ ions on the barite surface because these two mechanisms will always tend to make the surface electrically neutral.

B. Variation of Zeta Potential in Different Electrolyte Solutions

The zeta potential of barite and quartz was measured in solution with varying amounts of Ba^{++} ion (in chloride form) at several selected pH levels. (see Fig. 12) Fig. 12 shows that a positive change in zeta potential of barite always occurs with increasing Ba^{++} ion concentration. The surface potential of quartz reduced to zero as the Ba^{++} ion concentration is increased. The Ba^{++} ion is the potential determining ion for barite. Therefore, with increasing Ba^{++} ion concentration, some of the Ba^{++} ions in the solution phase will adsorb on the barite surface resulting in a positive surface potential. Reduction of zeta potential of quartz with increasing the Ba^{++} ion concentration results from the compression of the double layer.

The effect of oleate concentration on the zeta potential of barite was determined for three different initial pH conditions as shown in Fig. 13. The pH levels were chosen so that the initial surface charge was positive, zero, and negative. As may be observed in Fig. 13, the zeta potential of barite always becomes more negative with increasing concentration of Na-oleate in solution. The zeta potential of quartz does not show a consistent negative change with increasing oleate concentration. These experimental results indicate that the presence of oleate ions had a much greater influence on the zeta potential of barite than for quartz. Earlier workers interpreted the observed changes in zeta

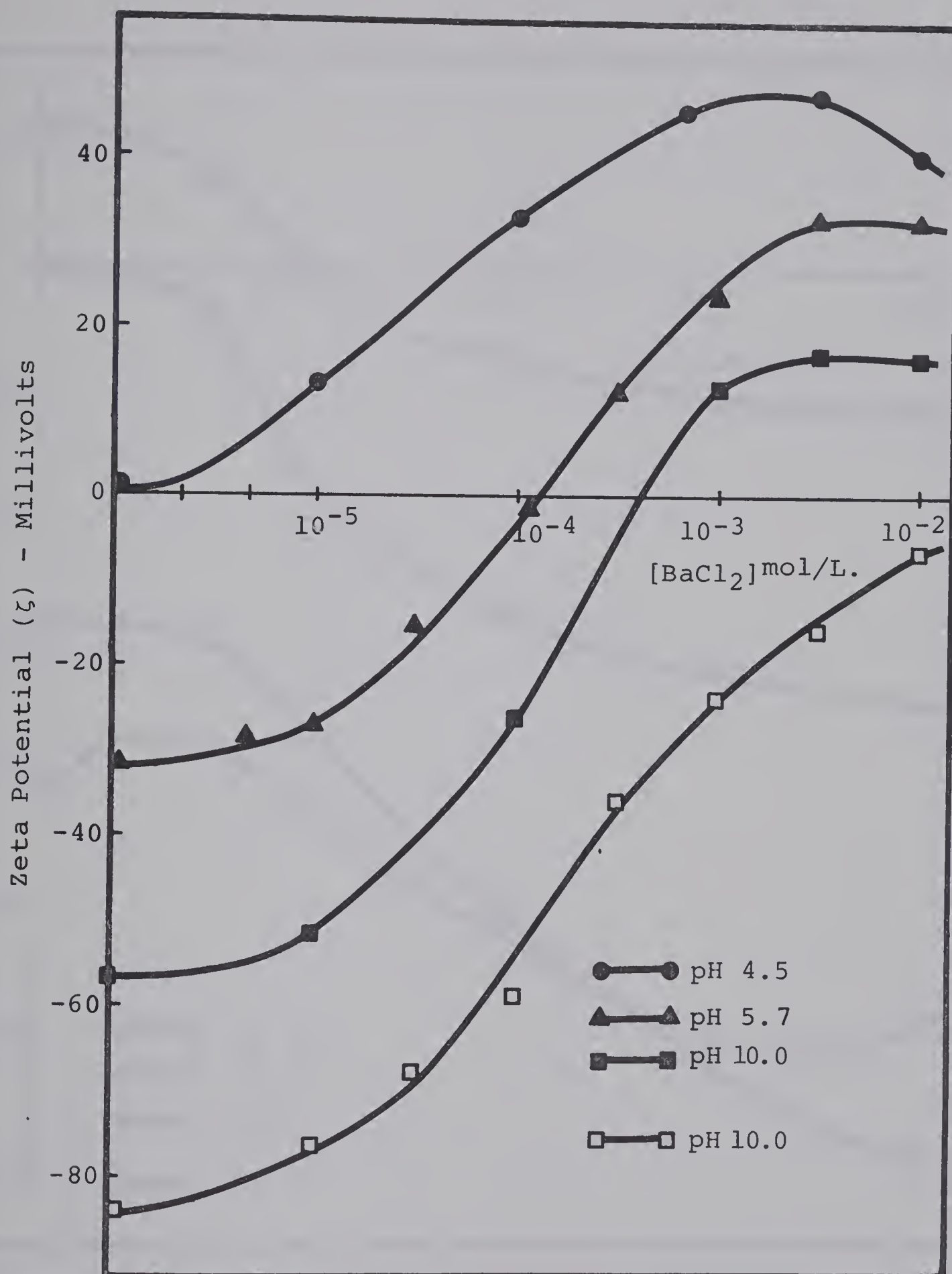


Fig. 12. Variation of Zeta Potential as a Function of the BaCl₂ Concentration (Filled Symbols: Barite, Open Symbols: Quartz)

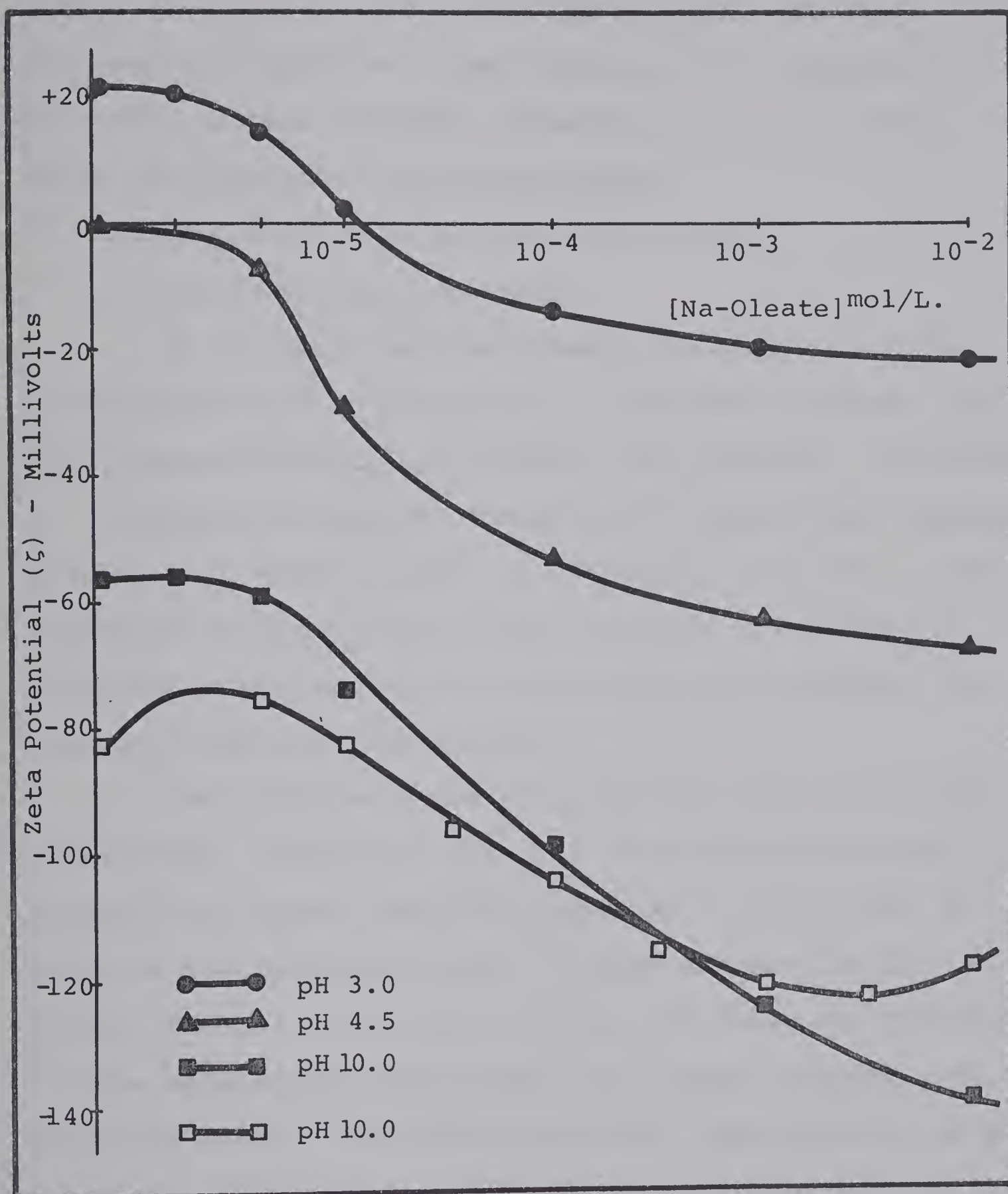


Fig. 13. Variation of Zeta Potential as a Function of Na-Oleate Concentration
(Filled Symbols: Barite, Open Symbols: Quartz)

potential which occurred upon the addition of a surface-active electrolyte, as due to hemimicelle formation.⁽¹²⁾⁽¹⁷⁾

The special attractive forces causing ionic association at the solid surface originate from the dispersion forces among the collector hydrocarbon chains.

2. Infrared Studies on Adsorbed Fatty Acids

A. C-H Stretching Vibrations

An infrared spectrum presents an analysis of the vibrational modes in molecules, it can often represent the most characteristic single feature of a molecule. Therefore, an infrared investigation can directly identify the adsorbed species on a solid surface. In addition, the state of the adsorbent surfaces prior to and following a treatment in collector solutions can be characterized by observing the changes in the infrared spectra.

The spectrum of the C-H stretching mode in a hydrocarbon chain is shown in Fig. 14. The unsaturated acids exhibit an infrared absorption band (A) at about 2995 cm^{-1} which is attributable to the C-H bonds adjacent to the C=C double linkage. This band is similar in shape and position for the unsaturated fatty acids, i.e. oleic, linoleic and linolenic acids. The intensity of this band relative to the methylene C-H stretching bands (D and E) increases with the degree of the unsaturation. With increasing unsaturation in the hydrocarbon chain, the intensity of the C-H stretching bands for methylene groups is weakened. Accordingly, the observed changes of relative intensity of band A to band D

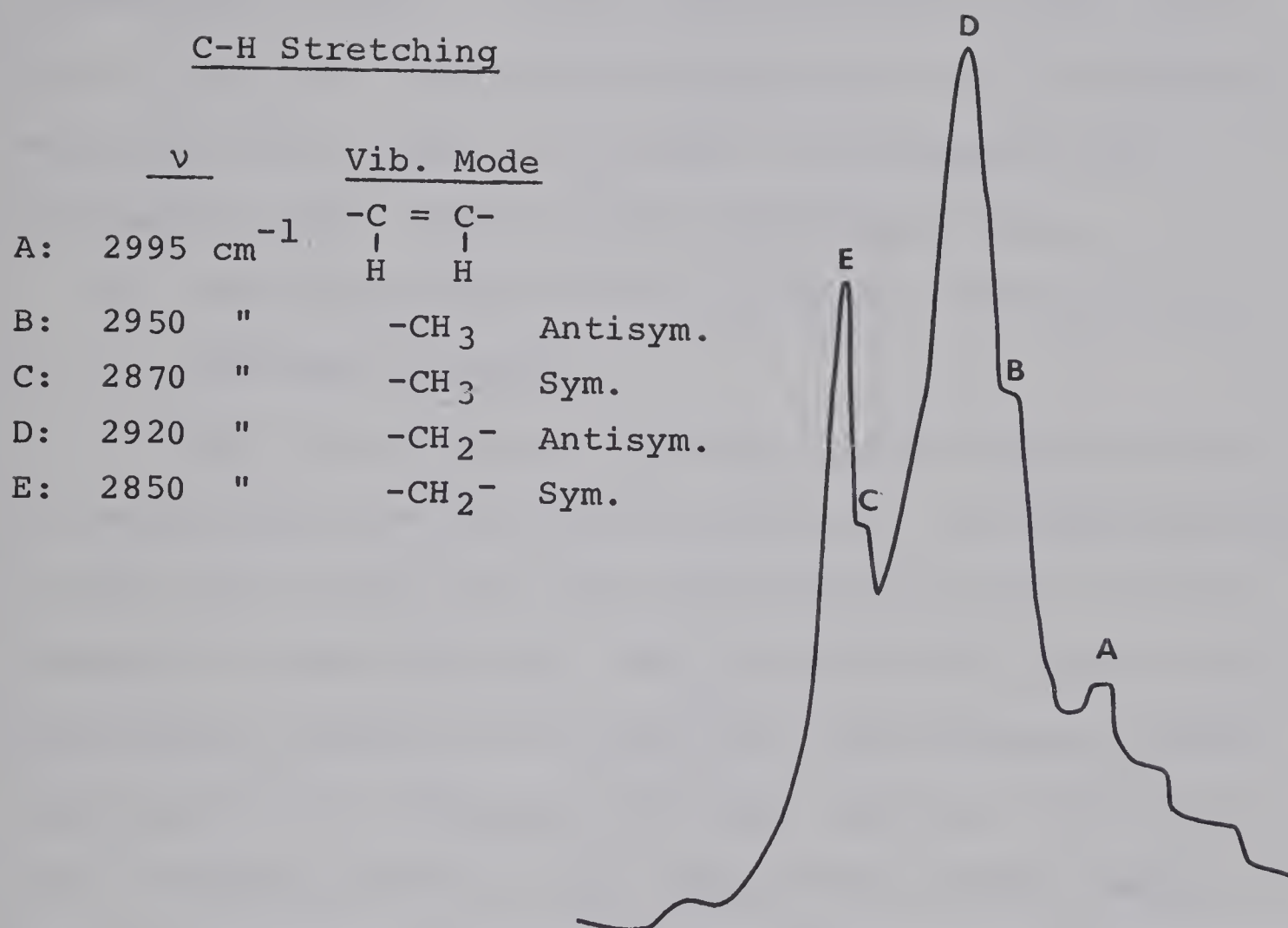


Fig. 14. Typical Infrared Spectrum of an Unsaturated Fatty Acid.

can be used to evaluate the degree of unsaturation of a hydrocarbon chain.⁽³⁶⁾ The adsorption bands at 2950 and 2870 cm^{-1} (B and C) represent the antisymmetry and symmetry stretching vibration bands of the terminal methyl group in a hydrocarbon chain. For the saturated fatty acids, the band at 2995 cm^{-1} (A) does not appear and the relative intensity of band D and E to B and C is increased with increasing carbon length in the hydrocarbon chain.

B. Infrared Spectra of Various Kinds of Fatty Acids Adsorbed on Barite

The C-H stretching spectra of fatty acids adsorbed on barite particles are shown in Fig. 15. Infrared spectra of pure fatty acids were also taken for C-8 and C-12 and compared to adsorbed ones. For the pure fatty acids with hydrocarbon lengths of C-8 and C-12, the adsorption bands representing the methylene vibration (2920 and 2850 cm^{-1}) have a higher intensity than that of the terminal methyl group. As would be expected, the C-H band due to an adjacent C=C linkage does not appear in the spectra of the unadsorbed fatty acids. In the spectra of the n-saturated fatty acids adsorbed on barite, a new band appears. This new band corresponds to C-H stretching which is adjacent to a C=C group. For the fatty acids with a carbon length less than 12, the methylene group adsorption bands (2920 and 2850 cm^{-1}) are also diminished upon adsorption. A sudden increase in the adsorption intensity of adsorbed fatty acids above C-14 carbon length was observed. This increase may be attribu-

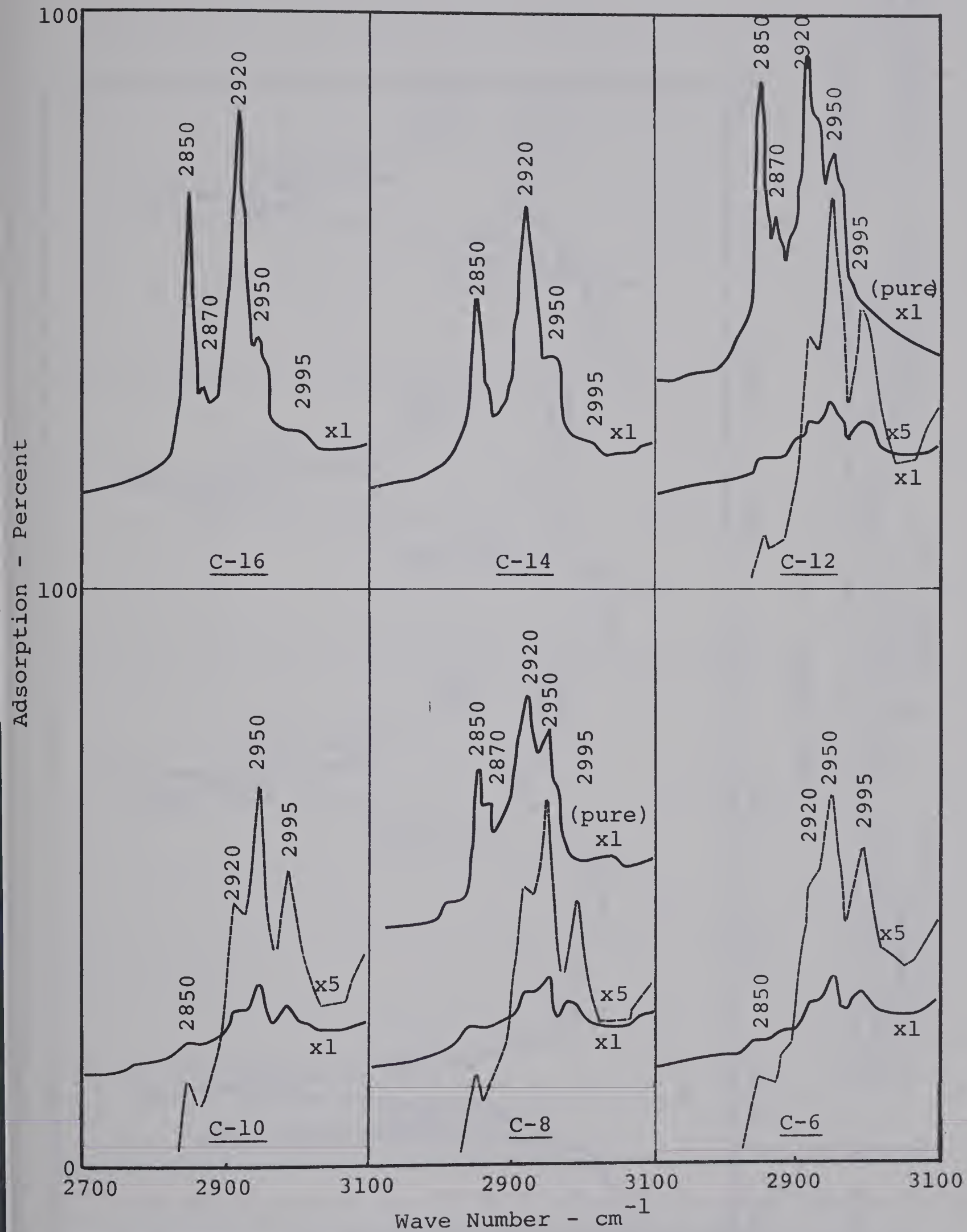


Fig. 15. Infrared Spectra of N-saturated Fatty Acids Adsorbed on Barite (Conc. = 10^{-3} mole/L, pH = 10.0)

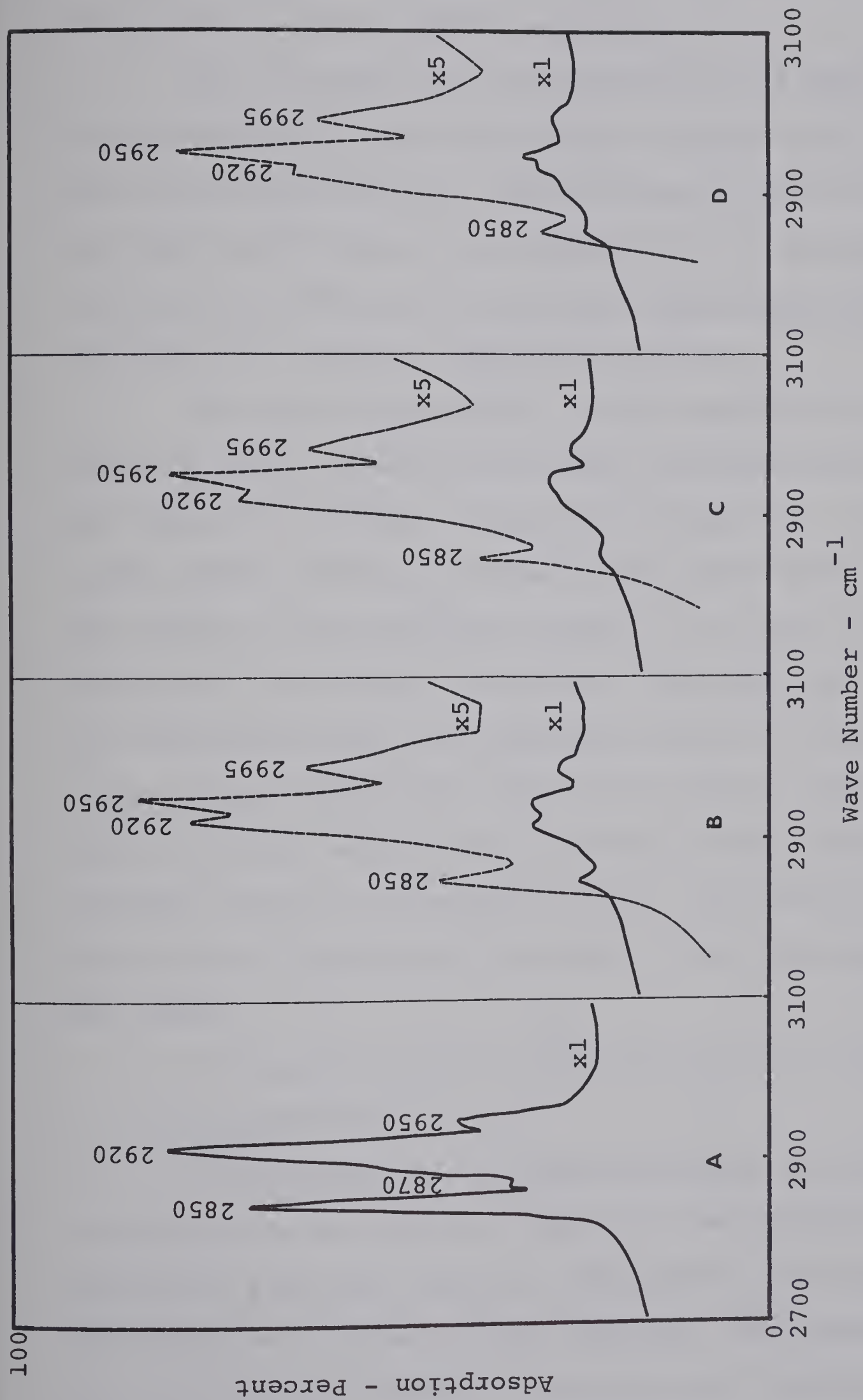


Fig. 16. Infrared Spectra of C-18 Fatty Acids with Various Number of Double Bonds in Their Hydrocarbon Chain (Conc.=10⁻³mole/L, at pH 10.0)
 A: Na-Stearate (no double bond) B: Na-Oleate (1 double bond) C: Na-Linoleate (2 double bonds) D: Na-Linolenate (3 double bonds)

table to the low solubility of the long hydrocarbon chain fatty acids in their sodium-salt form.

Fig. 16 shows the infrared spectra of adsorbed unsaturated fatty acids all having a carbon length of 18 but with differing structure. With increasing unsaturation of the hydrocarbon chain, the intensity due to methylene groups is decreased, whereas, the terminal methyl group bands (2950 and 2870 cm^{-1}) show no appreciable changes.

The above experimental results provide strong evidence of direct interaction between the hydrocarbon chains and the barite surface. From this interaction, new carbon-carbon double bonds are formed in the hydrocarbon chain at the expense of the methylene groups. H-C bonds in a methylene group are covalent in nature. Therefore, the electrons in a methylene group are localized around the central carbon atom. When a hydrocarbon chain is in contact with the surface of barite, some of the electrons in the surface $\text{SO}_4^{=}$ ions probably shift to the hydrogen atoms. This shift of electrons will lead to formation of C=C bonds in the adsorbed hydrocarbon chain.

C. Infrared Spectra of Adsorbed Oleate in Different Concentrations

Infrared spectra of adsorbed oleate in different concentrations are shown in Fig. 17. The methylene group adsorption bands are gradually diminished with decreasing concentration of oleate in the solution. The overall intensity of adsorption bands is increased only slightly by the

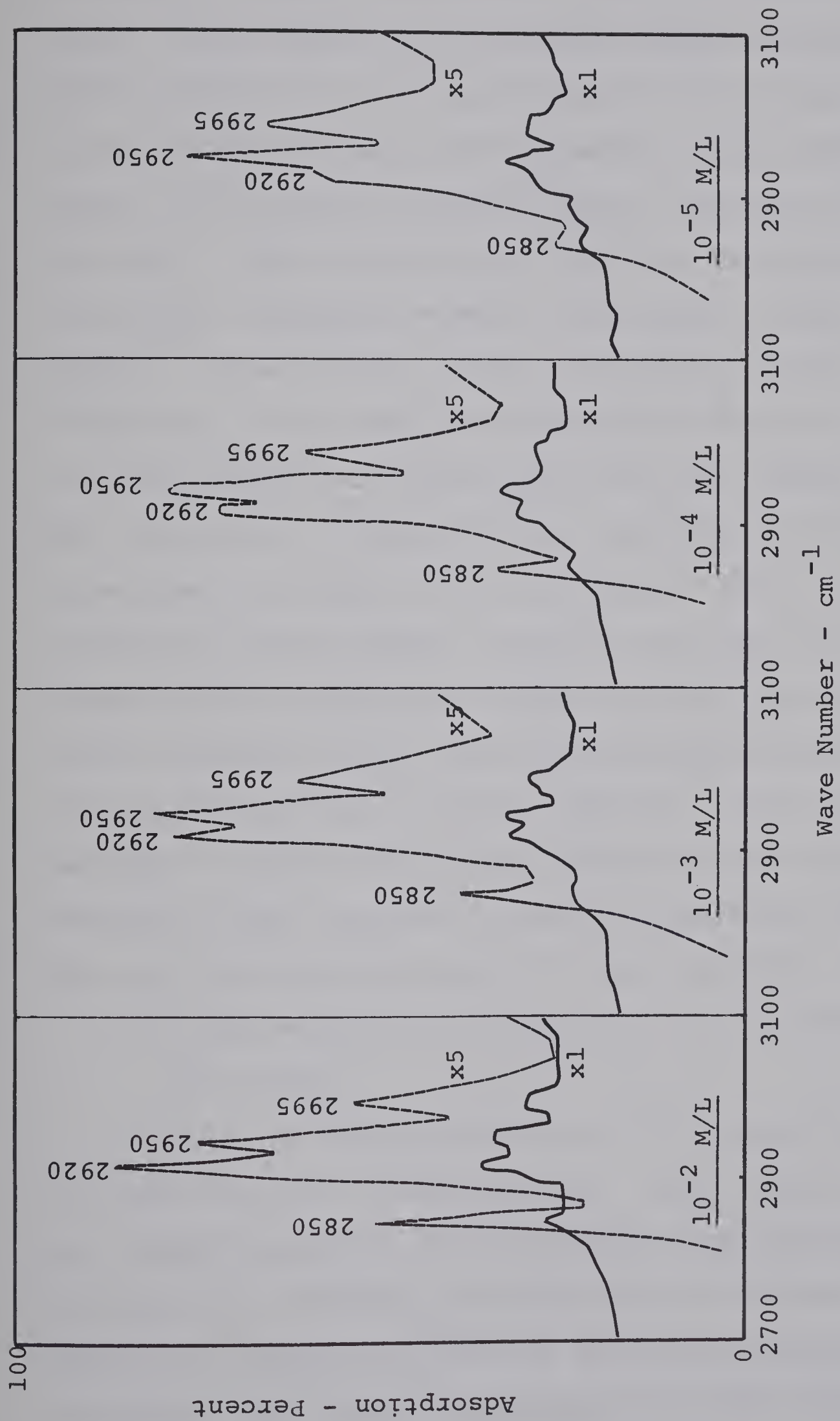


Fig. 17. Infrared Spectra of Na-Oleate Adsorbed on Barite in Different Concentrations
(at pH 10.0)

increase of oleate concentration from 10^{-5} to 10^{-2} mole/litre. There seems to be a strong interaction between the barite surface and the oleate species of the first adsorbed layer leading to double bond formation in the hydrocarbon chain. This reaction proceeds until a monolayer coverage is obtained. After formation of the first adsorbed layer, the multilayer adsorption seems to take place by weak physical forces. These physical forces are made up of the attractive dispersion forces among the hydrocarbon chains and the electrostatic repulsive forces among the ionic collector heads. The net balance of these forces, repulsive and attractive, determines the depth of the multilayer. With a high concentration of oleate species, some of the oleate ions are hydrolyzed and this hydrolyzed neutral collector species would be easily adsorbed on the top of the monolayer since only very weak repulsive forces would be expected. This increase in adsorbed collector multilayer thickness would account for the observed slight increase in infrared adsorption intensity for the higher concentration of oleate species.

D. Infrared Spectra of Adsorbed Oleate at Different pH Levels

Fig. 18 shows the effects of H^+ ion on the adsorption of fatty acid on a barite surface. These spectra show that the overall intensity of the infrared adsorption bands increases with decreasing pH indicating an increase in the amount of adsorbed collector on the barite surface. This increase in the amount of adsorbed collector would be

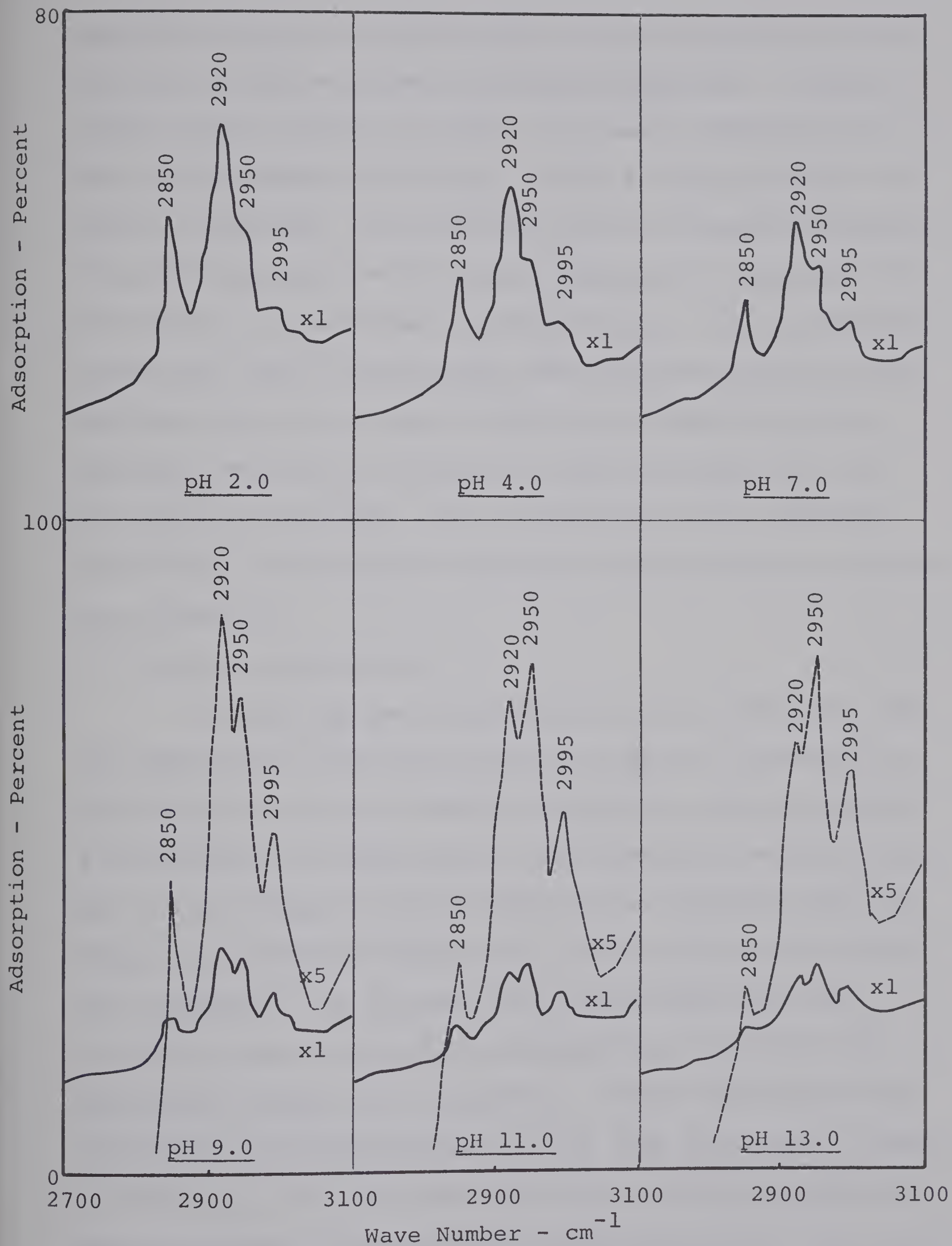


Fig. 18. Infrared Spectra of Na-Oleate Adsorbed on Barite in Different pH. (Na-Oleate: 10^{-3} mole/L)

expected, since at low pH levels, a high proportion of the collector would be present as neutral molecules. (The adsorbed oleate spectrum for $\text{pH} = 2$ is nearly identical to that of unadsorbed oleic acid.) With a high proportion of neutral molecules, the repulsive forces originating from the charged ionic heads would not be effective in limiting the thickness of the adsorbed collector layer. It is also observed that with increasing pH, the relative height of the infrared adsorption bands of the C-H in methylene group decreases, whereas the adsorption band resulting from the C=C group is increased. This observation again indicates that double carbon-carbon bonds are formed during the adsorption reaction.

3. Flotation Experiments

It has long been recognized in froth flotation that the hydrocarbon chain of a collector molecule provides the hydrophobicity to the normally hydrophilic mineral surface. A large amount of experimental and theoretical work has been done in an attempt to understand how the structure and the length of a collector hydrocarbon chain affects its collecting properties. It has been well established that the collecting power is normally increased by increasing the hydrocarbon length of a collector. On the other hand, the solubility of collectors having very long hydrocarbon chains is very low, with the result that their collecting power is sharply reduced. Unsaturation in the hydrocarbon chain also affects the collecting properties. It is believed that the

unsaturated fatty acids are normally better flotation collectors than their saturated homologues.⁽²⁾ With increasing unsaturation, a slight decrease in collecting power is generally observed.⁽¹⁸⁾

A. Flotation Recovery of Barite as a Function of the Concentration of Various Fatty Acids

Fig. 19 shows the recovery vs. the concentration of n-saturated fatty acids having different carbon lengths. For the experimental conditions used, the fatty acid with C-6 does not have any appreciable collecting power for the barite. With increasing carbon atoms in the hydrocarbon chain from 8 to 14, the collecting power increases almost 10-fold for every additional 2 carbon atoms. Above C-16, the collecting power drops sharply due to the reduced solubility.

Another interesting phenomenon observed in this experiment is that the flotation recovery is reduced when very high concentrations of long-chain n-saturated fatty acids (above C-14) are used. The commonly held explanation for this phenomenon has been the formation of a bimolecular layer with collector molecules in the second layer having their charged heads exposed to the liquid phase (see Fig. 3B).⁽¹⁾ This explanation, however, does not seem to be valid for the fatty acid-type collectors for the reasons already cited in Theoretical Review.

Fig. 20 shows the effect of unsaturation of the hydrocarbon chain on the collecting properties of fatty acids. Flotation recovery is reduced in the order of oleate, lino-

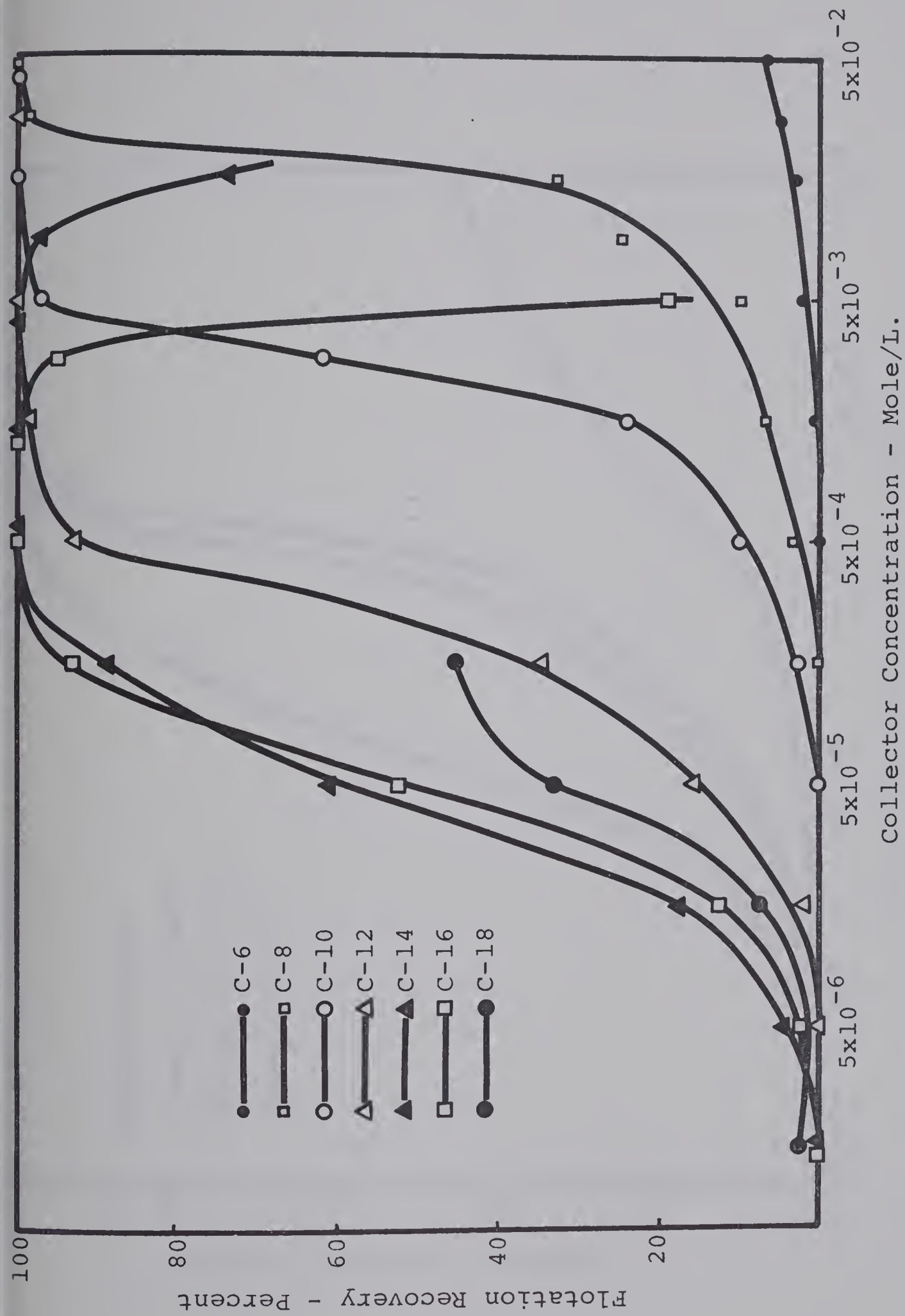


Fig. 19. Flotation Recovery of Barite as a Function of the Concentration of N-saturated Fatty Acids (at pH 9.5)

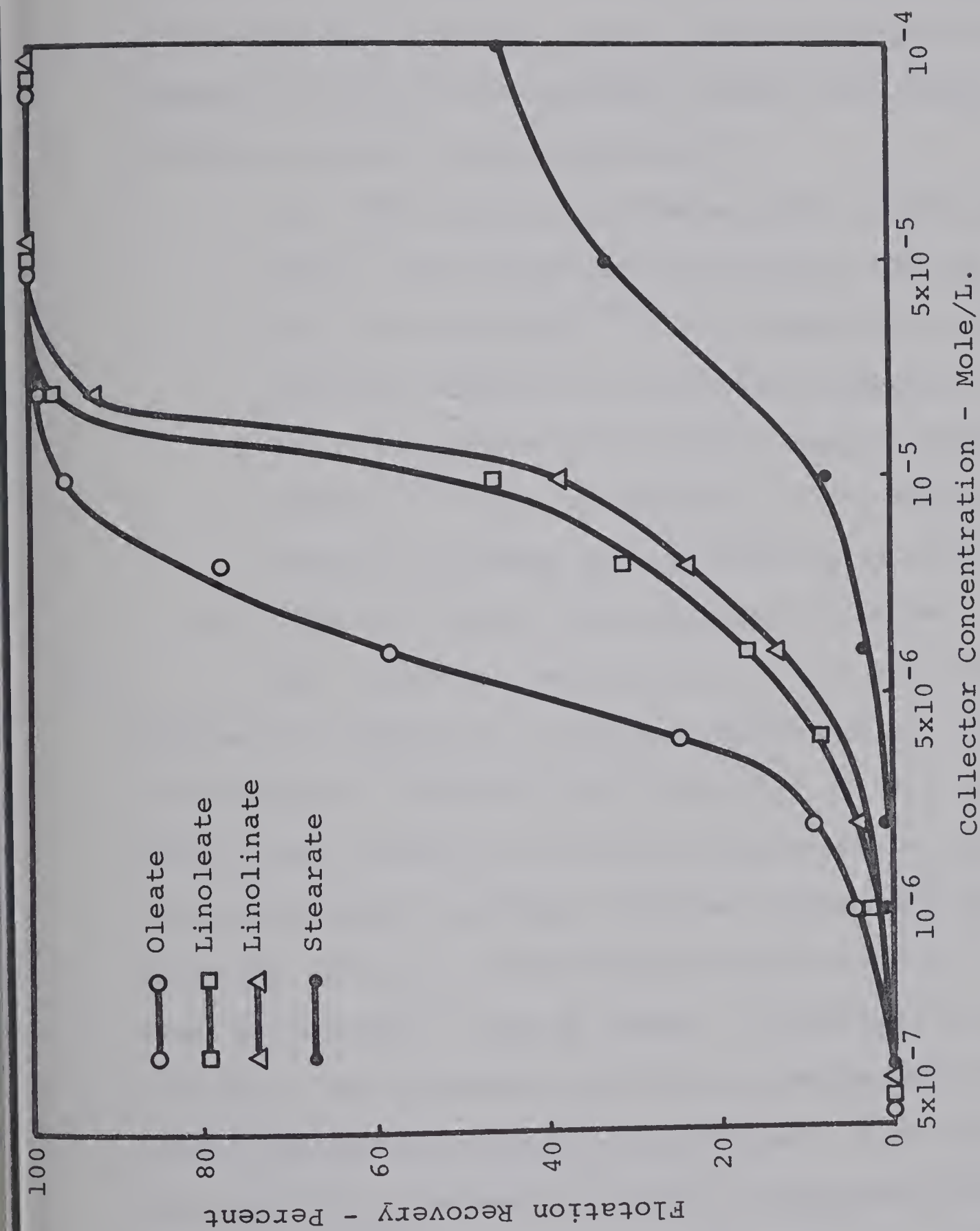


Fig. 20. Flotation Recovery of Barite as a Function of the Concentration of Unsaturated Fatty Acids with 18 Carbon Atoms (at pH 9.5)

leate and linolate. This order is not consistent but varies with the mineral used, and the flotation conditions employed for the tests.⁽¹⁸⁾⁽²⁴⁾⁽³⁹⁾ Generally oleic acid with one double bond has proven to be superior to both linoleic (two C=C) and linolenic (three C=C) acids. Two possible reasons can be considered:

(a) With increasing double bonds in the hydrocarbon chain, the susceptibility of the collector to oxidation is increased.⁽³⁹⁾ Any oxidation of the collector will reduce its collecting properties.

(b) The carbon-carbon double bond is polar in nature,⁽²³⁾ thus an increase in the number of these bonds will reduce the hydrophobicity of the collector.

B. Effects of pH on the Recovery of Barite

Fig. 21 shows the effects of pH on the flotation recovery of barite in a solution containing 10^{-4} mole/litre of Na-oleate. As can be seen from Fig. 21, the recovery of barite drops sharply as the pH is decreased to less than 4.0. Infrared studies regarding adsorbed oleate from different pH solutions (Fig. 18), show that the adsorption of oleate is greatly enhanced at low pH levels. Therefore, in acidic solutions, the flotation recovery is reduced even though overall adsorption density is increased. Peck and Wadsworth explained this phenomenon in terms of physical and chemical adsorption.⁽³²⁾ In their words, "a physically adsorbed collector species can not provide flotability to the solid surface while a chemisorbed species can". This explanation

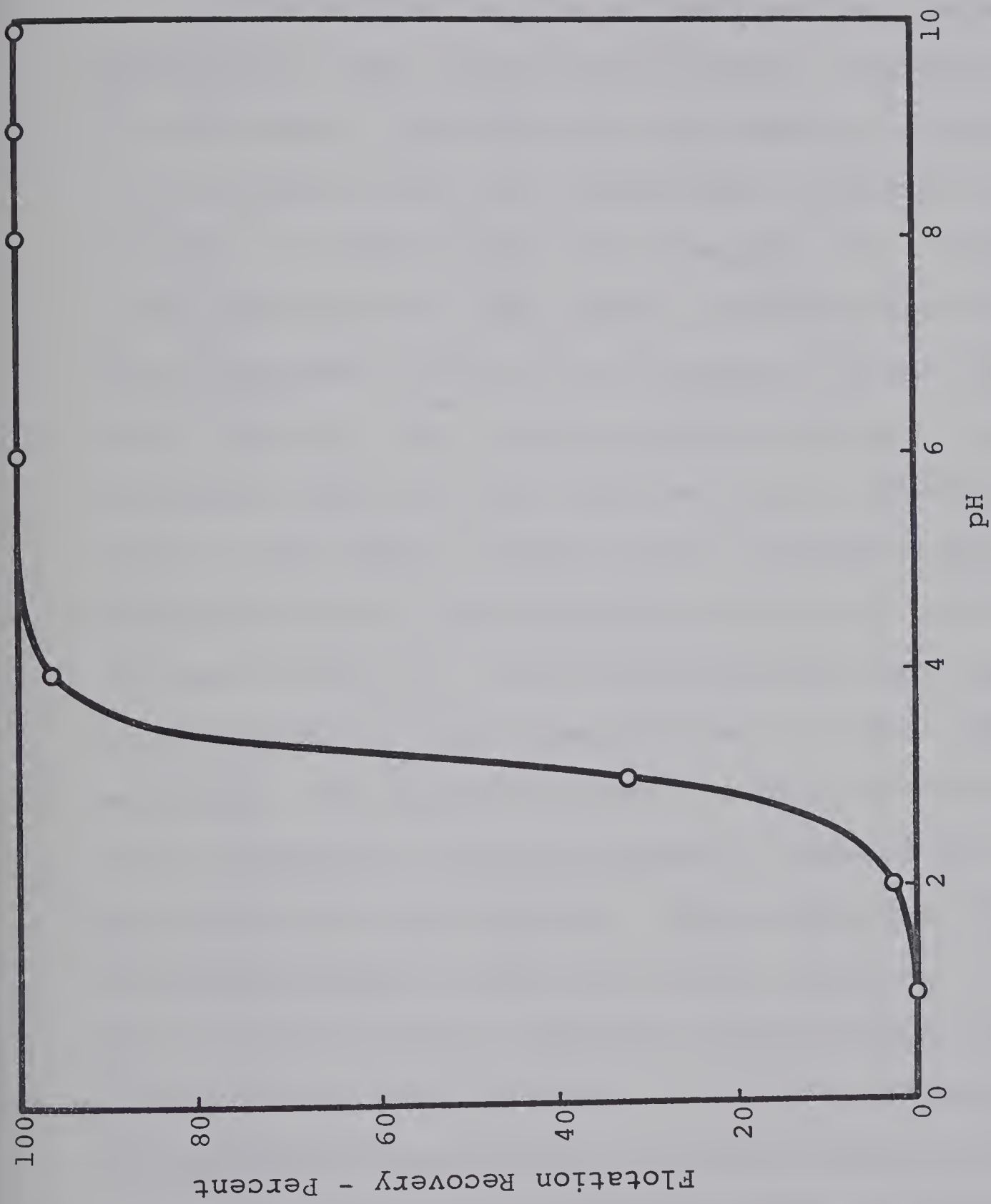


Fig. 21. Flotation Recovery of Barite as a Function of pH
(Na-Oleate, 10^{-4} mole/litre)

is, however, so general in nature that it provides little insight into the mechanisms involved in adsorption.

4. New Adsorption Model for Fatty Acid-Type Collectors

Theoretical considerations regarding the adsorption mechanism of fatty acid-type collectors, mentioned earlier in this thesis, proposed that the compact monolayer formation of collectors, with their polar heads attached to the solid surface, is rather unrealistic (see Fig. 3B). Infrared tests, performed for this thesis, confirmed the direct interaction between the collector hydrocarbon chain and the mineral surface. As a result of this evidence, a new collector adsorption model for the fatty acid-type collectors is proposed. This model, together with a schematic diagram of air bubble attachment on a collector-conditioned solid surface is given in Fig. 22. Fig. 22A illustrates what happens when the collector is highly ionized i.e. in highly alkaline solutions. The ionized collector species are held on the solid surface by a strong interaction between the hydrocarbon chains and the solid surface. These adsorption forces should be strong enough to keep the collector species on the surface over the electrostatic repulsive forces between the collector heads and the charged surface. In the second adsorbed layer, the repulsive forces among the charged collector heads will be greater than the weak attractive forces among the hydrocarbon chains. Therefore, in this situation, a thick multilayer formation appears to be very unlikely. When an air bubble approaches this collector-conditioned surface, the

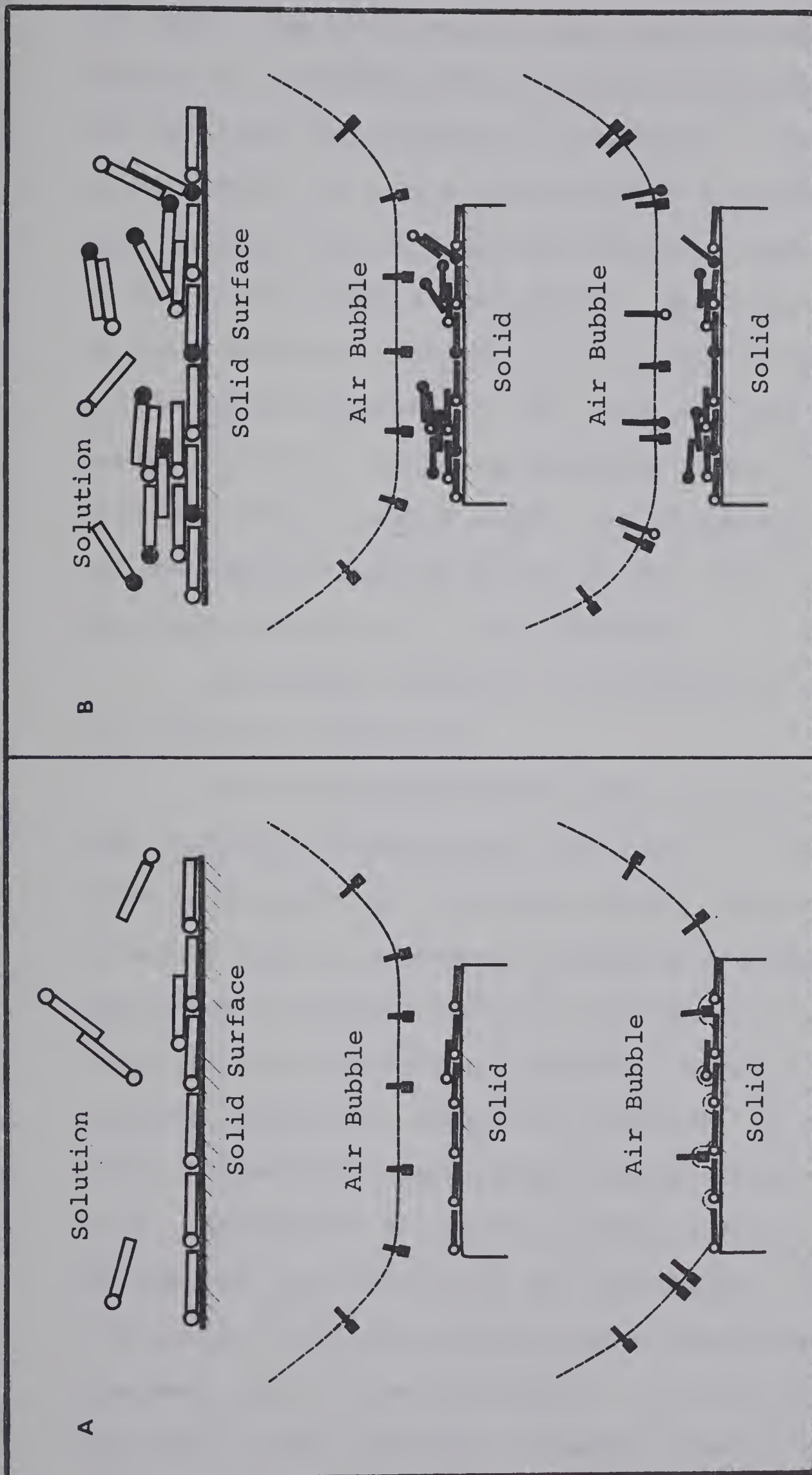


Fig. 22. Schematic Diagrams of Collector Conditioned Solid Surfaces and Air Bubble Attachment.

() Collector Ion Frother Molecule Neutral Collector

air bubble can make contact with the first adsorbed layer. Because of the hydrophobic nature of the hydrocarbon chains, the particles are amenable to flotation. (See Fig. 22A). In this model, the size ratio between the hydrocarbon chain and the polar head is expected to play a very important role in making the surface hydrophobic. The size of polar heads in fatty acids are same while the length of the hydrocarbon chains varies according to the structure and the number of carbon atoms in a collector molecule. For the fatty acids with less than 6 carbon atoms, the hydrophilic polar parts are predominant and therefore, do not give any flotability even when adsorbed on a solid surface.

Multilayer formation of collector is favorable under the following conditions:

(a) a long hydrocarbon chain collector is used, (b) high collector concentration, and (c) at a low pH. With these conditions, the repulsive forces among the polar collector heads are reduced considerably because of the appearance of neutral molecular species in the adsorbed layer. Therefore, the multilayer formation is possible. With increasing adsorption density of collector, an electrical charge accumulation take place causing further adsorption to cease. Attractive forces and repulsive forces among collector species are balanced in the multilayer, and consequently continuous adsorption and desorption takes place in the outermost part of the multilayer. If an air bubble approaches, only some of the outermost collector species would be picked

up by the air bubble, leaving the particle in solution unaffected by the bubble contact (see Fig. 22B).

SUMMARY AND CONCLUSIONS

Experimental results obtained by various kinds of experimental techniques enable certain conclusions to be drawn regarding the collecting mechanisms of fatty acid-type collectors.

The prime results obtained from the experimental techniques employed for this thesis are as follows:

- (1) Surface potential of barite and quartz is dependant upon the pH of the solution. Barite will specifically adsorb H^+ ions from the solution making its surface positively charged at pH levels less than 4.5. The surface potential of quartz is determined by the dissociation of surface silicic acids.
- (2) Surface potential of barite shows enormous changes with different concentration of Ba^{++} ion and Na-oleate. It is obvious that the Ba^{++} ion is the potential-determining ion for barite. The oleate ion seems to adsorb on the barite surface by specific adsorption forces. The surface potential of barite becomes more negative with increasing oleate concentration.
- (3) Infrared spectra for adsorbed fatty acids on a barite surface showed that there is a direct interaction between the hydrocarbon chains and the solid surface. New C=C double bonds are formed in the hydrocarbon chains of the first adsorbed layer at the expense of the $-CH_2-$ (methylene) groups. The surface of barite seems to act as a catalyst for this reaction.

- (4) In ionic form, the collector species adsorb on the barite surface as a thin monolayer, while with increased amounts of neutral molecular species in solution, a multilayer formation take place.
- (5) Flotation experimental results show that the fatty acids with carbon length 6, or less, do not show any collecting power for barite. The collecting power increases with increasing the hydrocarbon chain length.
- (6) The collecting power of a fatty acid decreased with increasing unsaturation in the hydrocarbon chain.
- (7) The flotability of barite is very low in acidic solutions even though the overall collector adsorption density is very high.

Based upon the above experimental results, a new model for fatty acid type collector adsorption has been proposed. In this new model, the importance of the interaction between the hydrocarbon chains and the solid surface is emphasized. The main difference between this model and previously proposed ones is that the new model predicts that even in high concentrations, the collector species are lying parallel to the surface. Previous models proposed that the collector species are erect, with their hydrocarbon chains extended away from the solid surface forming a compact monolayer.

This new collector adsorption model serves to explain the following characteristic collecting properties of fatty acid-type collectors:

- (1) The carbon length in fatty acid-type collectors is very crucial on their collecting properties when compared with xanthate-type collectors.
- (2) Reduction of flotability in very concentrated collector solutions.
- (3) In some cases, anionic collectors will be adsorbed on a negatively charged mineral surface.
- (4) Nonselective collecting properties.

REFERENCES

- (1) Billett, O.F. and Ottewill, R.H., "The Dependence of Contact Angle on the Adsorption of Surface Active Agents", Wetting S.C.I. Monograph No.25, Soc. of Chem. Indus., 1967.
- (2) Buckenham, M.H. and Mackenzie, J.M.W., "Fatty Acids as Flotation Collectors for Calcite", AIME Trans., Vol. 220, p.450, 1961.
- (3) Castellan, G.W., Physical Chemistry, Addison-Wesley Pub. Co., 1966.
- (4) Clark, A., Theory of Adsorption and Catalysis, Academic Press, New York and London, 1970.
- (5) Cook, M.A., "Hydrophobicity Control of Surfaces by Hydrolytic Adsorption", Hydrophobic Surface edited by Fowkes, F.M., 155th Meeting of Amer. Chem. Soc. in 1968, Academic Press, New York, 1969.
- (6) Cook, M.A. and Nixon, J.C., "Theory of Water-Repellent Films on Solids Formed by Adsorption from Aqueous Solutions of Heteropolar Compounds", J. of Phys. and Coll. Chem., Vol.445, 1950.
- (7) Deju, R.A. and Bhappu, R.N., "Relationship of Chemical Reactions Between Water and A Silicate Bed to the Flow Equation" AIME Trans., p.115, June, 1970.
- (8) Eischens, R.P. and Pliskin, W.A., Advance in Catalysis, Vol.IX, p.662, Academic Press, New York, 1957.
- (9) Eitel, W., The Physical Chemistry of Silicates, Univ. Chicago Press, Chicago, 1954.

- (10) Eyring, E.M. and Wadsworth, M.E., "Differential Infrared Spectra of Adsorbed Monolayer-n-Hexanethiol on Zn Minerals", AIME Trans., Vol.205, p.531, 1956.
- (11) French, R.O., Wadsworth, M.E., Cook, M.E. and Cutler, I.B., "The Quantitative Application of Infrared Spectroscopy to Studies in Surface Chemistry", J. of Phys. and Chem., Vol.58, p.805, Oct., 1954.
- (12) Fuerstenau, D.W., Froth Flotation, 50th Aniv. Volume, AIME, New York, 1965.
- (13) Fuerstenau, D.W. and Modi, H.J., "Streaming Potentials of Corundum in Aqueous Organic Electrolyte Solutions", J. of Electrochem. Soc., Vol.106, p.336, 1959.
- (14) Fuerstenau, D.W., Metzger, P.H. and Seele, G.D., "How to Use This Modified Hallimond Tube", Eng. and Mining J., Vol.158, p.93, March, 1957.
- (15) Fuerstenau, M.C., Gutierrez, G. and Elgillani, D.A., "The Influence of Sodium Silicate in Nonmetallic Flotation Systems", AIME Trans. Presented at the AIME Annual Meeting in New York, Feb., 1968.
- (16) Gaudin, A.M., Flotation, 2nd edition, McGraw-Hill Book Co., New York, 1957.
- (17) Gaudin, A.M. and Fuerstenau, D.W., "Quartz Flotation with Cationic Collectors", AIME Trans., Vol.202, 1955.
- (18) Gaudin, A.M. and Cole, R.E., "Double-Bond Reactivity of Oleic Acid During Flotation", Technical Note, AIME Trans., Vol.196, p.418, 1953.

- (19) Good, J.R., "Closing Discussion", Wetting, S.C.I. monograph No.25, Soc. of Chem. Indus., 1967.
- (20) Greenwood, N.N., Ionic Crystals, Lattice Defects and Non-stoichiometry, Butterworths Co., London, 1968.
- (21) Haned, H.S. and Owen, B.B., The Physical Chemistry of Electrolyte Solutions, Reinhold Pub. Corp., New York, 1943.
- (22) Iwasaki, I., Cooke, S.R.B., Harraway, D.H. and Choi, H.S., "Iron Wash Ore Slimes-Some Mineralogical and Flotation Characteristics", AIME Trans., Vol.223, p.97, 1962.
- (23) Iwasaki, I., Cooke, S.R.B. and Choi, H.S., "Flotation Characteristics of Hematite, Goethite, and Activated Quartz with 18 Carbon Aliphatic Acids and Related Compounds", AIME Trans., Vol.217, p.237, 1960.
- (24) Kivalo, R. and Lehmusvaara, E., "Investigation into the Collecting Properties of Some of the Compounds of Tall Oil", Trans. Intl. Mineral Dressing Cong., Stockholm, p.577, 1957.
- (25) Klassen, V.I. and Mokrousov, V.A., An Introd. to Theory of Flotation, English Trans., Butterworths Co., London, 1963.
- (26) Li, H.C. and deBruyn, P.L., "Electrokinetic and Adsorption Studies on Quartz", Surface Sci., Vol.5, p.203, 1966.
- (27) Long, R.P. and Ross, S., "An Improved Mass-Transport Cell for Measuring Electrophoretic Mobility", J. of

Coll. Sci., Vol.20, p.438, 1965.

- (28) Lyklema, J. and Overbeek, J.Th.G., "On the Interpretation of Electrokinetic Potentials", J. of Coll. Sci., Vol.16, p.501, 1961.
- (29) Lyons, J.W., "Sodium Tri(poly)phosphate in the Kaolinite-Water System", J. of Coll. Sci., Vol.19, p.389, 1964.
- (30) Mining Assoc. of Canada, "Mining: What It Means to Canada", 1971.
- (31) Morrison, R.T. and Boyd, R.N., Organic Chemistry, 2nd edition, Allyn and Bacon Inc., Boston, 1966.
- (32) Peck, A.S. and Wadsworth, M.E., "Infrared Spectrophotographic Study of Oleate Adsorption on Fluorite, Barite and Calcite", Proceedings VII Intl. Min. Proc. Cong., 1964.
- (33) Poling, G.W., "Infrared Studies of Adsorbed Xanthates", Ph.D. Thesis, Univ. of Alberta, 1963.
- (34) Schmut, R., "Zeta Potential Measurements", Chem. and Phys. of Interfaces, Amer. Chem. Soc. Symp., p.95, 1965.
- (35) Senett, P. and Oliver, J.P., "Zeta Potential", Chem. and Phys. of Interfaces, Amer. Chem. Soc. Symp., p.75, 1965.
- (36) Sinclair, R.G. and McKay, A.F., "The Infrared Absorption Spectra of Unsaturated Fatty Acids and Esters", J. of Amer. Chem. Soc., Vol.74, p.2578, 1952.
- (37) Smolik, T.J., Harman and Fuerstenau, D.W., "Surface Characteristics and Flotation Behavior of Alumino-

silicates", AIME Trans., Vol.235, p.367, 1966.

- (38) Stigter, D. and Overbeek, T.Th.G., "The Energetics of Highly Charged Spherical Micelles as Applied to Na-Dodecyl Sulfate", Proc. 2nd Intl. Cong. of Surface Activity, Vol.1, p.311, Butterworths Co., London, 1958.
- (39) Sun, S.C., "Single Mineral Flotation with Linolenic, Linoleic, Oleic and Stearic Acids", AIME Annual Meeting, Feb., 1959.
- (40) Sutherland, K.L. and Wark, I.W., Principles of Flotation, Australian Inst. of Mining and Metallurgy, Melbourne, 1955.
- (41) Taggart, A.F., Handbook of Mineral Dressing, John Wiley & Sons Inc., 1945.
- (42) Wadsworth, M.E., Conrady, R.G. and Cook, M.A., "Contact Angle and Surface Coverage for Potassium Ethyl Xanthate on Galena According to Free Acid Collector Theory", J. of Phys. and Coll. Chem., Vol.55, p.1219, 1951.

APPENDIX A

TABLE I - Zeta Potential vs pH

A. Barite

pH	Charge	Traveling Time (150 microns/sec)										T.Avg.* (sec)	ζ (mv)	S.D.** (mv)	
2.5	+	8.7	9.4	10.0	9.0	9.3	8.1	9.1	9.6	8.9	8.2	9.2	9.1	23.4	.5
3.0	+	10.5	10.2	12.6	10.3	11.5	10.9	10.4	11.2	10.6	10.2	9.3	10.7	19.8	.8
3.5	+	13.0	11.9	12.5	15.0	14.5	15.3	14.5	13.5	14.5	12.8	15.1	13.9	15.3	.9
4.0	+	15.0	15.0	18.8	21.2	18.4	22.0	21.4	20.1	24.0	16.2	19.8	19.3	11.0	.6
4.5		not measurable													
5.0	-	16.9	12.2	14.0	12.0	12.1	10.2	12.8	11.5	11.4	11.8	12.0	12.5	17.0	2.5
5.6	-	6.9	6.3	6.2	6.5	6.4	6.0	5.8	6.1	6.1	6.7	7.2	6.4	33.2	1.5
6.0	-	6.4	6.8	5.5	5.8	5.6	5.1	5.4	5.0	5.5	5.4	5.0	5.6	37.8	1.3
7.0	-	4.9	4.6	5.2	5.3	5.2	4.2	4.6	3.7	3.9	3.9	4.0	4.5	47.0	2.2
8.0	-	4.0	3.9	3.5	3.6	3.7	3.5	3.6	3.7	3.8	3.9	3.8	3.7	56.7	.3
9.0	-	3.3	3.8	3.9	3.7	3.7	3.8	3.2	3.8	3.3	3.8	3.9	3.7	58.0	.7
10.0	-	3.9	3.6	3.5	3.6	3.7	3.7	3.6	3.6	3.7	3.8	3.9	3.7	57.3	.2
10.5	-	3.5	3.6	3.5	3.8	3.6	3.7	3.3	3.5	3.7	3.4	3.3	3.5	59.8	.3
11.0	-	3.3	3.4	3.5	3.4	3.3	3.4	3.9	4.2	4.1	4.1	3.9	3.7	57.5	1.2
11.5	-	3.9	3.6	3.7	4.2	4.1	3.6	3.7	4.2	4.3	3.8	3.9	3.9	54.1	.5
12.0	-	4.8	4.6	4.6	4.3	4.7	4.5	4.7	4.6	4.9	4.3	4.6	4.6	45.1	.2

TABLE I - Zeta Potential vs pH (cont'd)

B. Quartz

pH	Charge	Traveling Time (150 microns/sec)										T.Avg.* (sec)	ζ (mv)	S.D.** (mv)	
		15.0	16.0	18.8	21.2	18.4	22.0	21.4	19.1	24.0	16.2				
2.0	-	15.0	16.0	18.8	21.2	18.4	22.0	21.4	19.1	24.0	16.2	19.8	19.3	11.0	.8
2.5	-	13.7	18.0	17.0	18.3	12.7	16.8	17.4	18.0	14.7	17.3	15.9	16.4	12.9	1.4
3.0	-	10.2	10.3	10.5	12.6	11.5	11.2	10.4	10.9	10.6	9.4	10.2	10.7	19.8	.3
4.0	-	6.3	6.0	6.2	5.5	5.5	4.8	4.6	5.1	5.2	4.5	5.4	5.4	39.4	1.8
4.5	-	3.6	3.7	3.9	3.6	3.7	4.1	4.2	4.2	4.3	3.8	3.9	3.9	54.1	.9
5.6	-	2.9	2.9	3.1	2.5	2.5	2.7	2.7	2.9	3.2	3.1	3.0	2.9	74.0	.4
6.0	-	2.7	2.7	2.8	2.6	2.3	2.4	2.8	2.2	2.6	2.6	2.2	2.5	83.3	.8
7.0	-	2.5	2.5	2.5	2.4	2.6	2.5	2.6	2.3	2.3	2.4	2.7	2.5	85.3	.2
8.0	-	2.2	2.2	2.3	2.4	2.0	2.3	2.2	2.4	2.6	2.4	2.4	2.3	91.2	.6
9.0	-	2.3	2.5	2.6	2.4	2.3	2.3	2.1	2.4	2.2	2.2	2.3	2.3	90.8	1.2
10.0	-	2.6	2.7	2.5	2.5	2.7	2.6	2.5	2.6	2.3	2.7	2.4	2.6	82.9	.6
11.0	-	2.4	3.1	2.5	2.4	2.6	2.8	2.6	2.7	2.4	2.6	2.3	2.6	82.0	2.2
12.0	-	3.0	2.8	3.2	3.3	3.2	2.8	2.9	2.7	2.8	2.9	2.9	3.0	71.7	.4

Remark: Voltage Gradient : 10 volt/cm

* Time Average

** Standard Deviation

TABLE II - Zeta Potential vs BaCl₂ Concentration

A. Barite

pH	Conc. (mol/L)	Ch.	Traveling Time (150 microns/sec)											T.Avg.* (sec)	ζ (mv)	S.D.** (mv)
	0		not measurable													
4.5	10 ⁻⁵	+	19.9	12.8	15.0	17.3	14.3	13.5	18.6	15.1	13.5	14.8	18.3	15.7	13.4	2.9
	10 ⁻⁴	+	6.2	4.8	6.9	6.6	6.9	6.2	6.2	5.8	6.4	6.7	7.3	6.4	33.3	1.4
	10 ⁻³	+	4.6	4.4	4.8	4.9	5.0	5.1	4.3	4.7	4.5	4.6	4.2	4.7	45.5	1.2
	5x10 ⁻³	+	4.5	4.5	3.8	5.1	3.2	5.7	5.9	4.6	3.8	3.8	4.2	4.5	47.4	2.3
	10 ⁻²	+	4.6	4.7	5.1	5.2	4.0	4.1	6.0	6.4	6.6	6.7	4.7	5.3	40.1	2.4
5.7	0	-	7.1	7.3	6.7	6.7	6.8	7.8	5.8	6.1	6.7	5.8	6.7	6.7	31.7	2.1
	10 ⁻⁶	-	6.4	7.0	7.4	7.8	8.1	6.6	7.6	8.2	7.2	6.6	7.5	7.3	28.9	1.8
	10 ⁻⁵	-	7.8	8.6	8.4	8.0	7.7	6.7	7.4	8.0	7.9	7.3	7.3	7.7	27.3	.9
	5x10 ⁻⁵	-	13.0	14.0	15.1	14.8	12.6	15.4	11.9	13.2	13.8	14.0	14.1	13.8	15.3	.8
	10 ⁻⁴	-	not measurable													
10.0	5x10 ⁻⁴	+	14.7	18.0	19.8	18.5	16.9	18.8	18.4	18.6	14.2	17.5	16.9	17.5	12.1	1.2
	10 ⁻³	+	8.8	7.3	11.6	9.5	8.3	7.2	8.5	11.0	7.8	9.5	10.8	9.1	23.2	3.5
	5x10 ⁻³	+	6.9	6.0	6.2	6.5	6.4	5.8	5.8	6.1	6.1	6.7	7.0	6.3	33.5	.4
	10 ⁻²	+	6.1	5.8	7.3	4.8	5.7	6.2	6.4	6.3	7.6	7.2	6.8	6.4	33.2	2.1
	0	-	4.0	3.9	3.5	3.6	3.7	3.5	3.6	3.7	3.8	3.9	3.8	3.7	56.7	.3
10.0	10 ⁻⁵	-	3.8	4.0	4.3	4.0	4.0	4.1	4.1	4.0	4.1	4.1	4.3	4.1	52.0	.2
	10 ⁻⁴	-	9.3	8.7	8.6	7.3	7.3	7.4	8.0	7.0	6.4	9.1	9.0	8.0	26.4	1.9
	10 ⁻³	+	13.7	18.0	17.0	18.3	12.7	16.8	17.4	18.0	14.7	17.3	15.9	16.4	12.9	1.7
	5x10 ⁻³	+	13.0	14.0	12.7	11.8	12.4	13.2	12.4	13.8	12.8	13.0	12.8	12.9	16.4	.3
	10 ⁻²	+	13.8	15.0	12.2	12.8	14.3	13.1	12.3	14.2	14.7	13.2	12.1	13.4	15.8	.6

TABLE II - Zeta Potential vs BaCl₂ Concentration (cont'd)

B. Quartz

pH	Conc. (mol/L)	Ch.	Traveling Time (150 microns/sec)										T.Avg.* (sec)	ζ (mv)	S.D.** (mv)	
	0	-	2.8	2.6	2.5	2.4	2.5	2.5	2.4	2.6	2.4	2.4	2.6	2.5	83.9	.4
	10 ⁻⁵	-	2.7	2.8	2.8	2.9	2.6	2.8	2.7	2.7	2.7	2.8	2.9	2.8	76.6	.2
	5x10 ⁻⁵	-	2.8	3.1	3.1	3.4	3.2	3.2	3.1	3.2	3.1	3.0	3.0	3.1	68.0	.3
	10 ⁻⁴	-	3.4	3.7	3.7	3.6	3.4	3.7	3.5	3.5	3.6	3.6	3.8	3.6	58.9	.2
10.0	5x10 ⁻⁴	-	5.8	5.2	6.3	5.0	6.7	6.5	5.3	5.9	6.0	6.2	5.4	5.9	36.2	1.2
	10 ⁻³	-	7.3	8.1	9.4	10.4	8.5	9.0	9.2	8.8	7.6	9.0	9.3	8.9	23.9	1.4
	5x10 ⁻³	-	13.4	12.6	10.0	10.0	11.0	14.6	15.4	16.4	14.5	15.0	16.6	13.6	15.6	4.0
	10 ⁻²	-	not measurable													

Remark: Voltage Gradient : 10 volt/cm

* Time Average

** Standard Deviation

TABLE III - Zeta Potential vs Na-Oleate Concentration

A. Barite

pH	Conc. (mol/L)	Ch.	Traveling Time (150 microns/sec)										T.Avg.* (sec)	ζ (mv)	S.D.** (mv)	
3.0	0	+	9.6	9.2	10.6	9.5	12.2	8.6	10.9	10.4	9.0	10.2	10.6	10.1	21.0	1.3
	10 ⁻⁷	+	12.6	10.3	10.9	10.4	9.6	10.0	9.6	9.8	11.2	10.3	10.5	10.5	20.2	.9
	10 ⁻⁶	+	18.0	16.0	15.8	14.2	15.7	12.8	13.0	16.5	13.6	16.4	18.0	15.5	13.7	1.8
	10 ⁻⁵		not measurable													
	10 ⁻⁴	-	13.2	16.0	14.8	14.5	12.4	15.4	15.6	18.7	16.0	14.8	15.4	15.2	14.0	1.5
4.5	10 ⁻³	-	10.4	9.2	8.6	13.6	9.5	12.2	12.6	9.9	10.8	11.2	10.4	10.8	19.7	2.6
	10 ⁻²	-	8.8	9.3	11.6	8.6	9.5	7.3	11.0	9.1	9.0	8.0	8.9	9.2	23.0	2.2
	0		not measurable													
10.0	10 ⁻⁷		not measurable													
	10 ⁻⁶	-	32.0	24.0	41.0	40.0	36.0	35.0	37.0	38.0	40.0	42.0	28.0	35.7	5.9	3.2
	10 ⁻⁵	-	6.4	7.0	7.4	7.8	8.2	6.6	7.6	8.2	7.2	6.6	7.5	7.3	28.9	.9
	10 ⁻⁴	-	4.2	4.2	4.2	3.6	3.8	4.0	3.9	4.4	3.8	3.9	3.8	4.0	53.1	.5
	10 ⁻³	-	3.7	3.5	4.0	3.0	3.1	2.9	2.5	3.2	3.3	3.8	4.0	3.4	63.0	2.6
10.0	10 ⁻²	-	2.9	3.1	3.1	3.1	3.2	3.2	3.1	3.1	3.3	3.2	2.8	3.1	68.2	1.5
	0	-	3.9	4.2	4.2	3.8	3.6	3.7	3.4	3.6	3.8	3.8	3.4	3.8	56.3	.6
	10 ⁻⁷	-	3.9	3.8	3.8	3.5	3.7	3.7	3.7	3.7	3.8	4.1	3.9	3.8	56.0	.2
	10 ⁻⁶	-	3.8	3.7	3.7	3.9	3.7	3.4	3.6	3.3	3.4	3.5	3.6	3.6	58.8	.3
	10 ⁻⁵	-	3.3	3.3	2.8	3.0	3.2	2.8	2.9	2.7	2.8	2.8	2.9	3.0	71.7	.7
10.0	10 ⁻⁴	-	2.2	2.6	1.9	2.2	2.2	2.3	2.0	2.0	2.3	1.9	2.1	2.2	98.4	1.1
	10 ⁻³	-	1.9	1.9	1.7	1.7	1.7	1.6	1.6	1.6	1.6	1.8	1.7	1.7	123.7	.4
	10 ⁻²	-	1.5	1.5	1.8	1.5	1.5	1.6	1.5	1.5	1.4	1.4	1.5	1.5	139.1	5.5

TABLE III - Zeta Potential vs Na-Oleate Concentration (cont'd)

B. Quartz

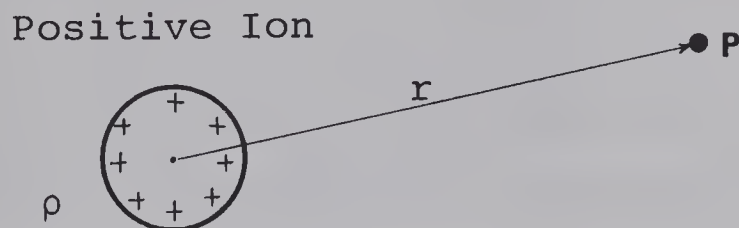
pH	Conc. (mol/L)	Ch.	Traveling Time (150 microns/sec)										T.Avg.*		S.D.**	
													(sec)	(mv)	(mv)	(mv)
10.0	0	-	2.4	2.6	2.4	2.6	2.5	2.6	2.7	2.7	2.5	2.5	2.6	2.6	82.9	.2
	10^{-6}	-	2.8	2.9	3.0	3.0	2.8	2.9	2.9	2.9	2.7	2.6	2.7	2.8	74.5	.3
	10^{-5}	-	2.6	2.7	2.5	2.2	2.8	2.2	2.6	2.7	2.6	2.4	2.8	2.6	82.9	.8
	5×10^{-5}	-	2.2	1.9	2.1	2.0	2.1	2.3	2.0	2.3	2.4	2.5	2.3	2.2	96.6	.8
	10^{-4}	-	2.0	1.8	1.9	2.0	2.1	1.9	2.4	2.2	2.0	2.0	1.9	2.0	104.7	.9
	5×10^{-4}	-	1.7	1.7	1.7	1.8	1.9	1.9	1.8	1.8	1.8	1.9	1.9	1.8	116.9	.3
	10^{-3}	-	1.8	1.7	1.8	1.8	1.7	1.6	1.9	1.7	1.7	1.6	1.8	1.7	121.6	.4
	5×10^{-3}	-	1.9	1.7	2.0	1.7	1.5	1.6	1.5	1.6	1.6	1.7	1.8	1.7	125.2	.9
	10^{-2}	-	1.9	1.8	1.7	1.6	1.9	1.7	1.8	1.8	1.8	1.9	1.8	1.8	118.2	.4

Remark: Voltage Gradient: 10 volt/cm

* Time Average

** Standard Deviation

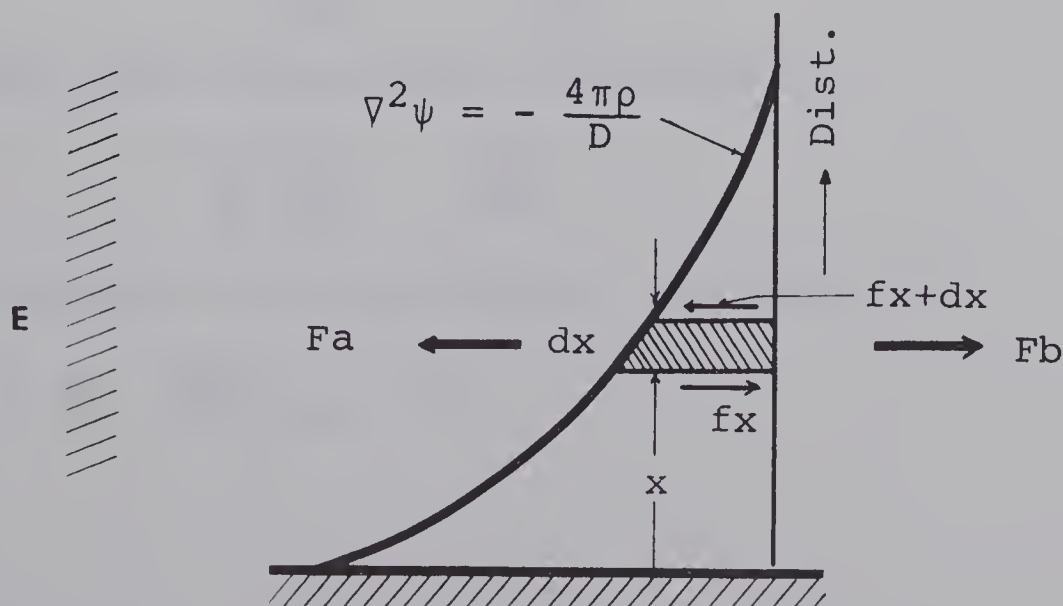
APPENDIX B

Derivation of the Smoluchowski Equation

Consider a point P at a distance r from the center of the ion. The potential ψ at the point P is related to the charge density ρ , the charge per volume, by the Poisson equation:

$$\frac{1}{r^2} \frac{d}{dr} (r^2 \frac{d\psi}{dr}) = - \frac{4\pi\rho}{D} \quad \text{or} \quad \nabla^2 \psi = - \frac{4\pi\rho}{D} \quad (1)$$

where ∇ is Laplace operator and D is the dielectric constant of the medium. If we assume that the liquid undergoes laminar flow, that its absolute viscosity, η , and dielectric constant, D , are uniform throughout the mobile part of the double layer, and that the thickness of the double layer is small compared to the radius of curvature of the surface, equation (1) can be changed to rectangular coordinates (x, y, z) , where only x -component is needed to be considered:



When an external field of strength E is applied, each volume element in a layer of liquid of thickness, dx , at a distance x from the surface, will experience a force:

$$F_a = E \cdot \rho \cdot dx \quad (2)$$

At steady state, the side of the layer at a distance x from the surface will be retarded by a frictional force given by:

$$f_x = -\eta \left(\frac{dv}{dx} \right)_x \quad (3)$$

where v is the liquid velocity; the side at a distance $x + dx$ from the surface will be accelerated by a force:

$$f_{x+dx} = \eta \left(\frac{dv}{dx} \right)_{x+dx} \quad (4)$$

Net friction force on the layer is:

$$F_b = \eta \left(\frac{dv}{dx} \right)_{x+dx} - \left(\frac{dv}{dx} \right)_x \quad (5)$$

At steady state the total force on the layer is zero, therefore:

$$E \cdot \rho \cdot dx = \eta \left(\frac{d^2v}{dx^2} \right) dx \quad (6)$$

For the x -component: $\nabla^2 \psi = \frac{d^2\psi}{dx^2}$

From equations (1) and (6) we obtain:

$$-\frac{ED}{4\pi} \frac{d^2\psi}{dx^2} = \frac{d^2v}{dx^2} \quad (7)$$

Integrating from shear plane to infinity:

$$-\frac{ED}{4\pi} \frac{d\psi}{dx} = \eta \frac{dv}{dx} + C \quad (8)$$

where C is zero from the boundary condition of

$$\left(\frac{d\psi}{dx} \right)_{x=\infty} = 0; \quad \left(\frac{dv}{dx} \right)_{x=\infty} = 0.$$

The second integration yields:

$$-\frac{ED}{4\pi} \cdot \psi = \eta v + C' \quad (9)$$

From the condition that at $x = \infty$, $\psi = 0$ and $v = v_e$ (the electrophoretic velocity), and at the shear plane, $v = 0$ and $\psi = \zeta$, then equation (9) becomes:

$$v_e = \frac{DE\zeta}{4\pi\eta} \quad (10)$$

or,

$$\zeta = \frac{4\pi\eta v_e}{DE} \quad (11)$$

Equation (11) is known as the Smoluchowski Equation.

The Smoluchowski equation is derived on the assumption of laminar flow (Particle Reynolds Number < 0.1) and constancy of the viscosity, η , and the dielectric constant D within the double layer. Assumption of laminar flow is easily met in practice. Experimental and theoretical information concerning the viscosity and dielectric constant in the double layer is lacking at the present time. However, Likhlema⁽²⁸⁾ and Li⁽²⁶⁾ showed that the use of the bulk values of D and η can be justified for low surface potentials and low ionic strengths. Since, Smoluchowski equation was derived for a mathematically plane surface, the ratio between particle size and the thickness of the electrical double layer must be large enough to justify the use of this equation. In practice, the size of the particles range from 1 ~ 3 microns and the thickness of double layer is usually close to $10^{-2} \sim 10^{-3}$ microns.

On the basis of the theoretical analysis explained above, it can be concluded that the direct use of the Smoluchowski equation, without further corrections, is justified for the experimental conditions used in this project.

B30013